Chem. Ber. **118**, 3588–3619 (1985)

Water-Soluble Tetraoxa[n.1.n.1]paracyclophanes: Synthesis and Host-Guest Interactions in Aqueous Solution

François Diederich, Klaus Dick,* and *Dieter Griebel*

Max-Planck-Institut für medizinische Forschung, Abteilung Organische Chemie, Jahnstr. 29, D-6900 Heidelberg

Received October 18, 1984

The synthesis of water-soluble tetraoxa[n.1.n.1]paracyclophanes **1c–8c** and open-chained model compounds **14c** and **15c** is described. **1c–8c** possess differently sized cavities of pronounced hydrophobic character as binding site for apolar guests in aqueous solution. In **1c–8c**, spiropiperidinium rings locate the water-solubility providing quaternary ammonium nitrogens remote from the cavity. The synthesis of water-insoluble tetraoxa[n.1.n.1]paracyclophanes **18–22** is described. The geometry of host compounds **1c–8c** is discussed in terms of CPK molecular models. The comparison of the ^{1}H NMR spectra in $CDCl_3$ and [D_6]benzene of the macrocycles **19–22** with the spectra of the open-chained analogues **26a–c** and **28** did not indicate a specific cavity effect on „aromatic solvent-induced shift" (ASIS). – The aggregation behaviour of **1c–3c**, **8c** and **14c** in aqueous solution was studied by ^{1}H NMR spectroscopy and the critical micelle concentration (CMC) of these compounds was determined. – Below the CMC of host and guest, complexation in aqueous solution between hosts **1c–8c** and apolar guests was investigated by fluorescence and ^{1}H NMR spectroscopy. Host-guest association constants K_a ($l \cdot mol^{-1}$) for 1:1 complexes were determined from fluorescence titrations. ^{1}H NMR investigations with hosts **1c–3c** and differently sized guests demonstrated that geometrical host-guest complementarity is a prerequisite for complexation. Remarkable differences of the changes of the chemical shifts upon complexation ($\Delta\delta$) were observed for the protons of the guest in aqueous solutions of host **2c** and a series of *para*-substituted toluenes **33a–l**. The different $\Delta\delta$-values indicate different degree and strength of complexation and are best explained in terms of a considerable contribution of van der Waals interactions to the free energy of complexation.

Wasserlösliche Tetraoxa[n.1.n.1]paracyclophane: Synthese und Wirt-Gast-Wechselwirkungen in wäßriger Lösung

Die Synthese der wasserlöslichen Tetraoxa[n.1.n.1]paracyclophane **1c–8c** und der offenkettigen Vergleichsverbindungen **14c** und **15c** wird beschrieben. **1c–8c** besitzen Hohlräume von unterschiedlicher Größe und von ausgeprägt hydrophobem Charakter, welche potentielle Bindungszentren für unpolare Gastmoleküle in wäßriger Lösung darstellen. In **1c–8c** sind die Wasserlöslichkeit bewirkenden quartären Ammonium-Ionen über Spiropiperidiniumringe dem Hohlraum abgewandt angeordnet. Die Synthese der wasserunlöslichen Tetraoxa[n.1.n.1]paracyclophane **18–22** wird beschrieben. Die Geometrie der Wirtmoleküle **1c–8c** wird anhand von CPK-Molekülmodellen diskutiert. Der Vergleich der ^{1}H-NMR-Spektren in $CDCl_3$ und [D_6]Benzol der Makrocyclen **19–22** mit den Spektren der offenkettigen Analoga **26a–c** und **28** lieferte keine Hinweise auf einen speziellen „Hohlraum-Beitrag" zum „aromatic solvent-induced shift" (ASIS). – Das Aggregationsverhalten von

0009–2940/85/0909–3588 $ 02.50/0

1c–3c, 8c und **14c** in wäßriger Lösung wurde mit Hilfe der ^{1}H-NMR-Spektroskopie untersucht, und die kritische Micellarkonzentration (CMC) dieser Verbindungen wurde bestimmt. – Unterhalb der CMC von Wirt und Gast wurde die Komplexierung in wäßriger Lösung zwischen den Wirtmolekülen **1c–8c** und unpolaren Gastmolekülen mit Hilfe der Fluoreszenz- und ^{1}H-NMR-Spektroskopie untersucht. Die Assoziationskonstanten K_a ($l \cdot mol^{-1}$) der gebildeten 1:1-Wirt-Gast-Komplexe wurden über Fluoreszenz-Titrationen bestimmt. ^{1}H-NMR-Untersuchungen mit **1c–3c** und Gastmolekülen unterschiedlicher Größe zeigten, daß räumliche Wirt-Gast-Komplementarität eine Vorbedingung zur Komplexbildung darstellt. Bemerkenswerte Unterschiede der durch Komplexierung bedingten chemischen Verschiebungen ($\Delta\delta$) der Gastprotonen wurden in wäßrigen Lösungen von Wirt **2c** und einer Reihe *para*-substituierter Toluole **33a–l** beobachtet. Die unterschiedlichen $\Delta\delta$-Werte zeigen unterschiedliche Komplexierungsgrade und -stärken an und lassen sich am besten durch die Annahme beträchtlicher Beiträge der van-der-Waals-Wechselwirkungen zur freien Komplexbildungsenergie erklären.

Our research efforts during the past years[1–3] were directed towards the synthesis of water-soluble macrocyclic hosts[4–7] of the cyclophane type with hydrophobic cavities for the complexation of apolar organic guest molecules in aqueous solution. To mimic the binding of substrates by enzymes, antibodies and receptors and to contribute to a better understanding of intermolecular interactions in aqueous solution, especially of the so-called hydrophobic interactions[8–10], were major targets of our studies. Additional interest in this kind of artificial hosts was derived from the intriguing properties of the inclusion complexes formed between native and modified cyclodextrins and a wide range of guests in aqueous solution as well as in the solid state[11–14].

In this paper we report on the synthesis and properties of the first series of water-soluble macrocyclic hosts **1–8** that we prepared[1]. The results of these investigations have led to the rational design and synthesis of very efficient artificial hosts for the complexation of apolar, especially aromatic, guests in aqueous solution[2,3].

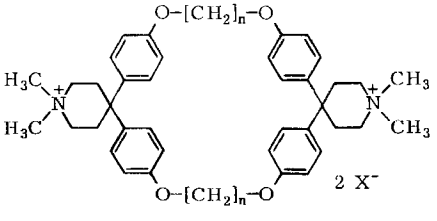

1a–c: n = 2
2a–c: n = 3
3a–c: n = 4
4a–c: n = 5

a: $X^- = FSO_3^-$
b: $X^- = BF_4^-$
c: $X^- = Cl^-$

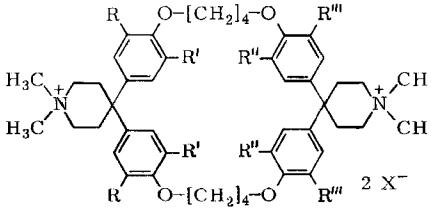

	R	R'	R''	R'''
5a–c	CH_3	H	H	H
6a–c	CH_3	CH_3	H	H
7a–c	CH_3	CH_3	CH_3	H
8a–c	CH_3	CH_3	CH_3	CH_3

In hosts **1–8** two diphenylmethane units, successfully introduced into host-guest chemistry by *Koga*[7,15], function as rigid aromatic spacers and cavity walls. The diphenylmethane units are bridged by α,ω-dioxaalkane chains of variable

chain-length (**1**–**4**). Water solubility at room temperature and neutral pH is provided by quaternary ammonium nitrogens located remote from the cavity. The apolar character of the binding site is thus not perturbed by strongly hydrated ionic centers as would be the case if the quaternary nitrogens were located in the macrocyclic skeleton surrounding the cavity. We have chosen spiropiperidinium rings to locate the quaternary nitrogens remote from the cavity[2b], since **9a**–**c** provide building blocks which combine the spiro-system with the diphenylmethane unit in a desired spatial arrangement.

Synthesis of the Macrocyclic Host Compounds

The synthesis of host compounds **1**–**8** started from building blocks **9a**–**c**, which could be easily prepared in large amounts by acid catalyzed condensation of *N*-acetyl-4-piperidone with two equivalents of the corresponding phenol (76–80%). Reaction of **9a**–**c** with large excess of the corresponding α,ω-dichloroalkanes in *n*-butanol in the presence of sodium hydroxide gave the cyclization components **10a**–**f** (72–88%).

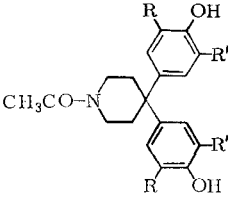

	R	R'
9a	H	H
b	CH_3	H
c	CH_3	CH_3

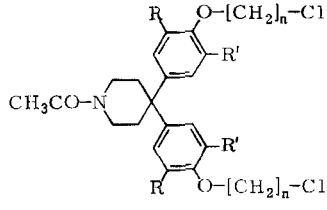

	n	R	R'
10a	2	H	H
b	3	H	H
c	4	H	H

	n	R	R'
10d	5	H	H
e	4	CH_3	H
f	4	CH_3	CH_3

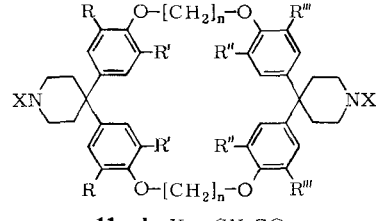

11a-h: X = CH_3CO
12a-h: X = H
13a-h: X = CH_3

	n	R	R'	R''	R'''
a	2	H	H	H	H
b	3	H	H	H	H
c	4	H	H	H	H
d	5	H	H	H	H
e	4	CH_3	H	H	H
f	4	CH_3	CH_3	H	H
g	4	CH_3	CH_3	CH_3	H
h	4	CH_3	CH_3	CH_3	CH_3

Cyclization of the dichlorides **10a**–**f** with the bisphenols **9a**–**c** in *n*-butanol in the presence of sodium hydroxide afforded the *N*-acetylated tetraoxa-

[n.1.n.1]paracyclophanes **11a–h** (7–15%). Alternatively the cyclizations were carried out in dimethylformamide with cesium carbonate as base (12–20%)[16]. Hydrolysis of the *N*-acetyl groups of **11a–h** using potassium hydroxide in 2-methoxyethanol afforded **12a–h** (80–95%) and Eschweiler-Clarke methylation gave the bis(*N*-methylpiperidine) macrocycles **13a–h** (58–81%).

Quaternization of **13a–h** to the bis(piperidinium fluorosulfonates) **1a–8a** was achieved with methyl fluorosulfonate ("magic methyl") in chloroform (82–95%). Addition of a saturated aqueous solution of sodium tetrafluoroborate to a concentrated aqueous solution of **1a–8a** led to the precipitation of the bis(piperidinium tetrafluoroborates) **1b–8b** (62–87%). Ion exchange chromatography (Dowex 1X8, Cl^-) starting from **1a–8a** provided the bis(piperidinium chlorides) **1c–8c** (68–91%) as colourless solids.

The bis(fluorosulfonates) **1a–8a** and the dichlorides **1c–8c** are very hygroscopic and a correct elemental analysis without water was only obtained for **1a**, **2a**, and **3a**. The bis(fluorosulfonates) and dichlorides take up rapidly stoichiometric amounts of water from the atmosphere (see Table 10). Elemental analysis indicated that the amount of water in the crystals did not change upon exposure of the crystals to laboratory air for one week. We prepared the bis(tetrafluoroborates) **1b–8b** since these salts are less hygroscopic. With the exception of **8b**, all bis(tetrafluoroborates) could be characterized free from water (see Table 10). The three types of salts differ considerably in their solubility. The dichlorides show the highest solubility in water followed by the bis(fluorosulfonates), whereas the bis(tetrafluoroborates) precipitate from aqueous solution. Similarly only **1a–8a** and **1c–8c** are readily soluble in alcohols. The bis(tetrafluoroborates) are easily soluble in acetonitrile and dimethylformamide. All salts are soluble in dimethyl sulfoxide. Extreme insolubility of all salts is expectedly observed in ethers and in apolar solvents like alkanes, benzene, or toluene.

The model compounds **14** and **15** for one half of the cavity of the macrocyclic hosts could be prepared by etherification of **9a** and **9c** with dimethyl sulfate to give **16a** (58%) and **16b** (96%) and subsequent conversions (**16** → **17** → **14** or **15**) using the procedures described above for the macrocyclic compounds.

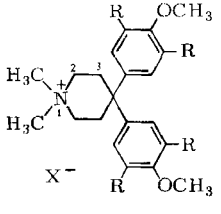

14a–c: R = H **a**: $X^- = FSO_3^-$
15a–c: R = CH_3 **b**: $X^- = BF_4^-$
c: $X^- = Cl^-$

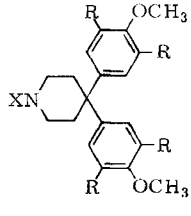

	X	R
16a	CH_3CO	H
b	CH_3CO	CH_3
17a	CH_3	H
b	CH_3	CH_3

Before accomplishing the synthesis of hosts with spiropiperidinium rings, we thought of introducing quaternary nitrogens via side chains attached to the aro-

matic rings of tetraoxa[n.1.n.1]paracyclophanes like **18**–**22**[17]. Side chains bearing quaternary nitrogens could possibly be introduced via functionalization of the benzylic methyl groups of **18** or via electrophilic substitution at the reactive aromatic carbon atoms *ortho* to the ether oxygens of **18**–**22**, followed by appropriate additional conversions.

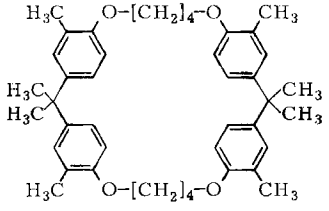

18

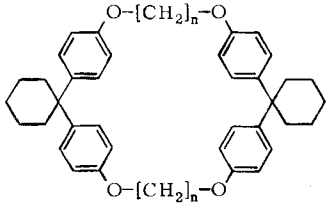

19: n = 2
20: n = 3
21: n = 4

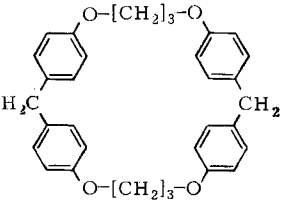

22

The synthesis of **18**–**22** proceeded in analogy to the preparation of **11a**–**h**. **18** was obtained from 2,2-bis(4-hydroxy-3-methylphenyl)propane (**23**)[18,19] and dichloride **24**. **19**–**21** were prepared from 1,1-bis(4-hydroxyphenyl)cyclohexane (**25**)[18,20] and **26a**–**c**[21]. Cyclization of bis(4-hydroxyphenyl)methane (**27**) with **28** gave **22**.

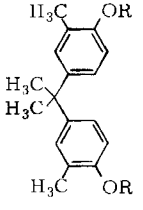

23: R = H
24: R = $-[CH_2]_4-Cl$

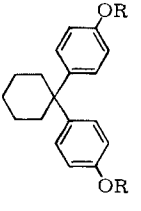

25: R = H
26a: R = $-[CH_2]_2-Cl$
b: R = $-[CH_2]_3-Cl$
c: R = $-[CH_2]_4-Cl$

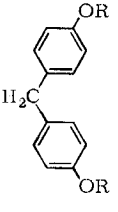

27: R = H
28: R = $-[CH_2]_3-Cl$

Geometry of the Macrocyclic Hosts 1–8

Figure 1 is a schematic drawing of the binding conformation of **3** supported by observations at CPK molecular models, by the ^1H NMR studies described below and in particular by the crystal structures of host-guest complexes formed by the bis(*N*-methylpiperidine) precursor **13c**[22]. A comparable binding geometry can also be assumed for the other water-soluble hosts of the series **1**–**8**.

The four benzene rings in the "face to face" conformation[6] are orientated perpendicular to the mean molecular plane of **3**. The four oxygens of the macrocyclic skeleton are turned outward away from the cavity, thus enhancing the hydrophobic character of the binding site. The maximum extensions of the cavities available for a guest molecule were estimated from CPK molecular models. In Figure 1 and Table 1, *A* is the distance (Å) between the spiro-carbon atoms of the two diphenylmethane units. *B* is the distance between parallel benzene rings and *C* the

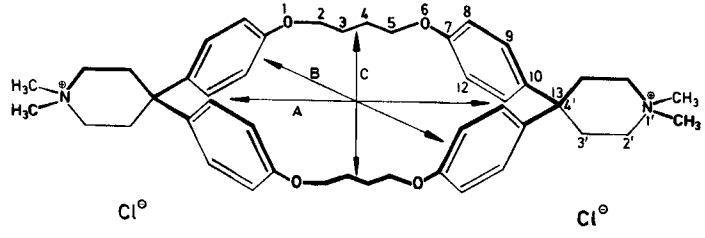

3c

Figure 1. Schematic drawing of the binding conformation of **3c**

Table 1. Estimated extensions of the cavities of **1**–**4**. For the meaning of *A*, *B*, *C* see Fig. 1

Host	*A* (Å)	*B* (Å)	*C* (Å)
1	≈5.4	≈4.8	≈4.5
2	≈6.3	≈5.4	≈4.5
3	≈7.5	≈6.6	≈4.8
4	≈8.7	≈7.5	≈4.8

distance between the aliphatic chains bridging the diphenylmethane units. An energetically favourable conformation of the aliphatic bridges with staggered hydrogen atoms of the methylene groups is assumed for these estimations[22]. According to the observations at CPK molecular models, the cavity of **1** could possibly enclose with a tight fit a benzene ring. A benzene ring should certainly fit into the cavity of **2**; possibly also an axially positioned naphthalene guest. An axially orientated naphthalene seems to be a good guest for **3**. **4** should enclose in its cavity a naphthalene guest also in equatorial position. In our studies we hoped to find out if estimates of host-guest complementarity from CPK molecular models can predict the experimentally observable complexation[23]. The depth of the cavities of **1**–**4** varies between ≈4 and ≈5.4 Å. The methyl groups attached to the diphenylmethane units of **5**–**8** deepen the cavity between these spacers; the depth of the cavity of **8** varies between ≈4 and ≈7.2 Å.

The *N*-methylpiperidine rings in the precursor molecules **13a**–**h** as well as the quaternized piperidinium rings in **1**–**8** adapt chair conformations[22]. By temperature dependent ^1H NMR spectroscopy (360 MHz, [D_4]methanol, tetramethylsilane (TMS) as internal standard) we could easily monitor the chair-chair inversion of the piperidinium rings of **8c** and **15c**. At 303 K, **15c** shows the following spectrum (cf. formula **15** for numbering of atoms): δ = 2.27 (s; 12H, Aryl-CH_3), 2.76 (mc; 4H, 3-H), 3.18 (s; 6H, N^+–CH_3), 3.43 (mc; 4H, 2-H), 3.70 (s; 6H, CH_3O), 7.04 (s; 4H, H_{arom}). At 209 K the number of signals had doubled: δ = 2.23 (s; 6H, Aryl-CH_3), 2.27 (s; 6H, Aryl-CH_3), 2.44 (t, $J \approx 14$ Hz; 2H, 3-H_{ax}), 3.07 (d, $J \approx 12$ Hz; 2H, 3-H_{eq}), 3.11 (s; 3H, N^+–CH_3), 3.20 (s; 3H, N^+–CH_3), 3.26 (t, $J \approx 14$ Hz; 2H, 2-H_{ax}), 3.51 (d, $J \approx 12$ Hz; 2H, 2-H_{eq}), 3.60 (s; 3H, CH_3O), 3.65 (s; 3H, CH_3O), 7.02 (s; 2H, H_{arom}), 7.15 (s; 2H, H_{arom}). Below 250 K the chair-chair inversion is slow on the 360 MHz

NMR time scale. Axial and equatorial 3-H, 2-H and N^+-CH_3 of the piperidinium ring in a rigid chair conformation show different chemical shifts. Our assignments of the protons of the piperidinium ring are based on the coupling pattern. The appearance of 2-H_{ax} and 3-H_{ax} at higher field than 2-H_{eq} and 3-H_{eq} is a consequence of the different orientation of these protons towards the C–C and the C–N bonds of the six-membered alicyclic skeleton. Furthermore, CPK molecular models indicate that axial 2-H and 3-H are orientated more into the shielding region of the adjacent benzene rings than equatorial 2-H and 3-H. Similarly the protons CH_3O, H_{arom} and Aryl-CH_3 of each of the two benzene rings now have a different orientation to the adjacent spiropiperidinium ring with its quaternary nitrogen atom and the counterion. Coalescence of the singlets of CH_3O and Aryl-CH_3 of **15c** was observed at T_c = 251 K. With $\Delta\nu$ (360 MHz) = 15.4 Hz (CH_3O) and $\Delta\nu$ = 15.8 Hz (Aryl-CH_3) the rate constant for the chair-chair inversion could be estimated as k_c = 68 s^{-1} and 70 s^{-1}, respectively, and the free enthalpy of activation was calculated as $\Delta G^{\ddagger}_{251}$ = 12.5 kcal · mol^{-1}.

The spectrum of the macrocyclic host **8c** exhibits a similar temperature dependency and from the coalescence of the singlets of N^+-CH_3 at T_c = 257 K ($\Delta\nu$ = 31.87 Hz) a rate constant of k_c = 141.59 s^{-1} and a free enthalpy of activation of $\Delta G^{\ddagger}_{251}$ = 12.4 kcal · mol^{-1} could be calculated. The $\Delta G^{\ddagger}$-values estimated at the coalescence temperatures (T_c between 250 and 260 K) of other suitable groups of protons of **15c** and **8c** are in good agreement with the given values.

Aromatic Solvent-induced Shifts (ASIS)

Most of the solvent shifts reported could be rationalized in terms of local dipole-induced dipole interactions between polar sites of the solute and the aromatic solvent molecules[24,25]. As consequence of these interactions, the aromatic solvent molecules take in the time average a particular, favoured orientation around the solute molecules, especially in the surroundings of polar sites. The anisotropy of the aromatic solvent molecules leads then to specific up- and downfield shifts of the protons of the solute.

In their studies of the complexation behaviour of hosts of the cyclophane type, *Jarvi* and *Whitlock* in 1982 were searching for a cavity effect on ASIS[17c]. A significant cavity effect leading to specific up- and downfield shifts of the protons of the host could be expected if the benzene solvent molecules can be accommodated in the molecular cavity of the host in a particular, favoured orientation. The authors proposed that the ASIS-values of their hosts support a cavity inclusion of the aromatic solvent molecules. The concept of specific cavity effects on ASIS seemed attractive to us. Such effects would provide a useful tool in determining specific host-guest interactions in the cavity.

We therefore looked at the aromatic solvent-induced shifts [Δ [ppm] = $\delta_{chloroform} - \delta_{benzene}$] of macrocycles **19**–**22** and their precursors **26a**–**c** and **28**. A special cavity effect should be recognized upon comparison of the ASIS-values of the macrocycles with the values of their open-chained analogues. Our results are summarized in Table 2. All compounds show considerable upfield shifts of the methylene protons of the aliphatic chains in α,β,γ or δ-position to the ether oxygens. The upfield shifts of the methylene protons of the open-chained analogues are larger than those of the macrocyclic compounds. The aromatic protons of all molecules show weaker upfield shifts than the protons of the aliphatic chains. The positions of the signals of the cyclohexane protons, not included in Table 2, are almost identical in both solvents. Although there are differences between the ASIS-values of the macrocyclic and the open-chained compounds, a specific cavity effect

was not observed in the considered series of compounds. Instead, the large Δ-values of the methylene protons near the ether oxygens and the chloride atoms are best explained by particular orientations of the benzene molecules around the aliphatic chains of the solutes as consequence of dipole-induced dipole interactions[24,26].

Table 2. Aromatic solvent-induced shifts (ASIS, Δ[ppm] = $\delta_{CDCl_3} - \delta_{[D_6]benzene}$) for particular groups of protons of solutes (80 MHz, 303 K, TMS int.)

Compound	OCH_2	OCH_2CH_2	Δ [ppm] $OCH_2CH_2CH_2Cl$ $OCH_2CH_2CH_2CH_2Cl$	H_o[a]	H_m[b]	$ArCH_2Ar$
26a	0.55	0.56		0.10	0.05	
19	0.33			0.03	0.07	
26b	0.41	0.48	0.44	0.03	0.00	
20	0.14	0.25		0.10	0.12	
26c	0.44	0.38	0.38 0.51	0.00	−0.04	
21	0.32	0.20		0.03	0.03	
28	0.43	0.46	0.43	0.06	0.05	0.07
22	0.17	0.24		0.04	0.20	0.14

[a,b] Aromatic protons *ortho* and *meta*, resp., to the ether oxygens of the solute.

Aggregation Behaviour in Aqueous Solution

The formation of stoichiometric molecular complexes between apolar hosts and guests in aqueous solution should be studied below the critical micelle concentration (CMC) of host and guest, i.e. with both components being in molecular dispersed form. Above the CMC, hydrophobic interactions, acting as driving force for stoichiometric complexation, can also lead to the segregated association of host and/or guest molecules or to formation of mixed aggregates with poorly defined orientation of host and guest, similar to micellar systems[5,27–29]. In order to avoid the interference of aggregation effects in our complexation studies, we investigated the aggregation behaviour of our hosts in aqueous solution. ^{1}H NMR was found to be the method of choice for this purpose[30]. The chemical shifts of the protons of **14c** and **1c**–**3c**[1] were plotted as a function of the concentration of these compounds. In the curves of a considered compound, a relatively well defined discontinuity was observed at approximately the same concentration. This concentration can be considered as the ^{1}H NMR critical micelle concentration of the compound. Below this value the chemical shifts are independent of concentration, above this value the chemical shifts become dependent on concentration. In addition, above the CMC strong line broadening of the signals, increasing with higher concentrations, is observed. Table 3 gives the CMC-values determined from these plots together with the maximum solubility of our compounds in aqueous solution. A large difference between water-solubility of a host compound in its molecular dispersed form and in its aggregated form is observed. The CMC of

3c[31] was determined independently by monitoring light scattering at 90° angle. A large increase of the relative intensity of scattered light was observed in aqueous solutions above [**3c**] = $2.5 \cdot 10^{-4}$ mol $\cdot$ l^{-1} (λ = 375 nm, T = 303 K).

Table 3. Critical micelle concentrations (^{1}H NMR, 303 K) and maximum solubilities in aqueous solution

Compound	CMC (mol $\cdot$ l^{-1})	Maximum solubility (mol $\cdot$ l^{-1})
14c	$6.0 \cdot 10^{-3}$	$>5 \cdot 10^{-1}$
1c	$2.5 \cdot 10^{-3}$	$\approx 2 \cdot 10^{-2}$
2c	$2.5 \cdot 10^{-3}$	$\approx 1 \cdot 10^{-1}$
3c	$1.6 \cdot 10^{-4}$ [31]	$\approx 1 \cdot 10^{-1}$
8c	$\leqslant 2 \cdot 10^{-5}$	$\approx 6 \cdot 10^{-2}$

The concentration dependency of the ^{1}H NMR spectra above the CMC is different for the various host compounds. Above the CMC, all protons of **1c** and **14c** move markedly upfield with increasing concentration. For example, at [**14c**] = 0.2 mol $\cdot$ l^{-1}, the signals of **14c** are shifted to higher field with regard to their positions below the CMC by +0.27 ppm (3′-H), +0.14 (N^+-CH_3), +0.21 (2′-H), +0.22 ($O-CH_3$), +0.28 (3-H) and +0.28 (2-H). The concentration dependency of the spectra of **2c** above the CMC differs from the one observed for **14c** and **1c**. In a concentration range close to the CMC all signals of **2c** move upfield. At [**2c**] $>10^{-2}$ mol $\cdot$ l^{-1}, a further upfield shift is observed only for the protons of the aliphatic bridges and for the protons around the quaternary nitrogens. At [**2c**] = 0.1 mol $\cdot$ l^{-1}, the signals of these protons are shifted upfield with regard to the positions below the CMC by +0.48 ppm (3-H), +0.39 (N^+-CH_3), +0.30 (2′-H), +0.37 (2-H). The chemical shifts of 3′-H and of the aromatic protons 7-H and 8-H however pass through a minimum value at [**2c**] $\approx 2 \cdot 10^{-2}$ mol $\cdot$ l^{-1}. At higher concentrations, these signals move downfield. A similar difference in the concentration dependency had been previously observed for the various groups of protons of host compound **3c**[1].

By introducing methyl groups at the diphenylmethane units, we hoped to reduce the aggregation tendency of our hosts and for **5c**–**8c** we expected a higher CMC-value than for **3c**. In surfactant chemistry, chain branching has been observed to lead to an increased CMC[29]. We found however that the methyl groups lowered the CMC-values of our host compounds. In the plot of the chemical shifts of the protons of **8c** as a function of concentration, no discontinuity in the curves was observed down to [**8c**] = $2.5 \cdot 10^{-5}$ mol $\cdot$ l^{-1}. From these curves, a CMC $\leqslant 2 \cdot 10^{-5}$ mol $\cdot$ l^{-1} can be estimated for **8c**. The concentration dependent shifts of the protons of **8c** again differ from those observed for **14c** and **1c**–**3c**. If passing from [**8c**] = $2.5 \cdot 10^{-5}$ mol $\cdot$ l^{-1} to [**8c**] = $6 \cdot 10^{-2}$ mol $\cdot$ l^{-1}, considerable upfield shifts are observed for the protons of the aliphatic bridges 2-H (+0.35) and 3-H (+0.40). Weaker upfield shifts are observed for the protons close to the aromatic rings of the diphenylmethane units: +0.19 (Aryl-CH_3), +0.10 (9-H)

and +0.08 (3′-H). The protons around the quaternary nitrogens are almost not shifted at all (< +0.04 ppm for 2′-H and N^+-CH_3). Based on these experiences, we introduced two more water-solubility providing quaternary ammonium ions remote from the cavity into our hosts and thus increased the CMC to a value of $7.5 \cdot 10^{-3}$ mol · l^{-1} for **29**[2].

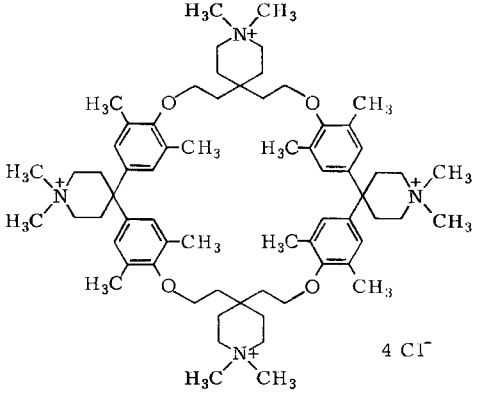

29

Figure 2 shows the strong temperature dependency of the ^1H NMR spectrum of **3c** above the CMC ([**3c**] = $2.4 \cdot 10^{-2}$ mol · l^{-1}) which is in contrast to the weak temperature dependency of the spectrum below the CMC. With [**3c**] = $1.0 \cdot 10^{-4}$ mol · l^{-1} the largest upfield shifts, when passing from 303 to 363 K, were only 0.04 ppm (9-H, 3-H). The shape of the curves for the various groups of protons of **3c** in the temperature plot (Figure 2) resembles the shape of the curves in the concentration plot[1].

The above-mentioned NMR experiments clearly show that large errors can be made by assigning observed changes of ^1H NMR chemical shifts to stoichiometric host-guest complexation if the spectra are recorded above the CMC of the host. The Δδ-values due to altered aggregation behaviour of the host in the presence of a guest can be important and in the same range or even higher than the changes due to molecular stoichiometric complexation.

The different changes in the chemical shifts of the various groups of protons of **2c**, **3c**[1], **8c** and **29**[2b] above the CMC suggest that in the aggregates these macrocycles do not take a random orientation. A favoured orientation of the macrocycles leading to specific structures of the aggregates can be admitted. The exchange between the macrocycles in the aggregates is fast since averaged signals are obtained in all NMR spectra. Further investigations are necessary in order to obtain a deeper insight into the aggregation behaviour of our hosts.

Host-Guest Complexation in Aqueous Solution

All work described in this section has been executed in aqueous solution below the CMC of the host compounds. The bis(piperidinium chlorides) **1c**–**8c** have been used exclusively.

Fluorescence studies. In view of the low CMC especially of the larger hosts (Table 3), host-guest interactions were first monitored by fluorescence spectroscopy, a sensitive analytical method in low concentration ranges. Hosts **1c–8c** exhibit no emission in aqueous solution under the conditions of the experiments described in this section.

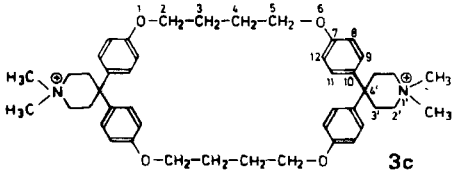

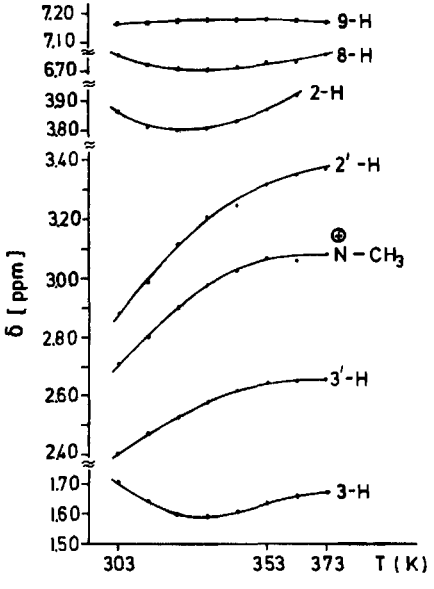

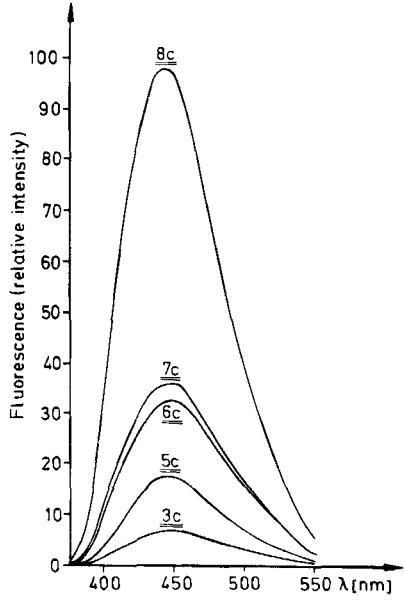

Figure 2 (left). Chemical shifts of the protons of **3c** as a function of temperature (80 MHz, D_2O, sodium 2,2,3,3-tetradeuterio-3-(trimethylsilyl)propionate (TSP) as external standard in D_2O; [**3c**] = $2.4 \cdot 10^{-2}$ mol $\cdot$ l^{-1})

Figure 3 (right). Fluorescence spectrum of TNS in aqueous solutions of **3c** and **5c–8c** (λ_{exc} = 360 nm, T = 292.5 K, $[H_0] = [G_0] = 1 \cdot 10^{-5}$ mol $\cdot$ l^{-1})

We studied the binding between **1c–4c** and 6-[(4-methylphenyl)amino]-2-naphthalenesulfonate (TNS, **30**), a guest known for the remarkable sensitivity of its fluorescence emission to the polarity of the environment[32]. In water, TNS exhibits a very weak fluorescence at $\lambda_{max} \approx 500$ nm, whereas in less polar environments a blue shift and a strong increase of the fluorescence intensity are observed. If in aqueous solution the apolar moieties of TNS are incorporated into a suitably sized hydrophobic cavity of a macrocyclic host, this is revealed by the

blue shift and the increase of the fluorescence intensity. The emission spectrum of TNS ([**30**] = $3.6 \cdot 10^{-6}$ mol · l^{-1}, λ_{exc} = 360 nm) in a $1 \cdot 10^{-4}$ molar aqueous solution of model compound **14c** was identical with the spectrum in pure water[1]. The emission intensity of TNS was slightly increased in a $1 \cdot 10^{-4}$ molar solution of the smallest host **1c**. The fluorescence intensity increased considerably when changing to $1 \cdot 10^{-4}$ molar solutions of the larger hosts **2c**–**4c**, the highest intensity being observed in the presence of **4c**. In addition, the emission maximum was shifted to shorter wave-length ($\lambda_{max} \approx 445-455$ nm) in these solutions. *Benesi-Hildebrand* type plots of the change in the fluorescence intensity of TNS upon addition of hosts **2c**–**4c** gave straight lines indicating 1:1 complexation in the considered concentration range, and the association constants K_a ($l \cdot mol^{-1}$) shown in Table 4 were calculated[33,2b].

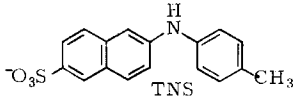

30

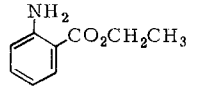

31

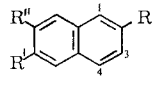

	R	R'	R''
32a	OH	OH	H
b	OH	H	OH
c	$SO_3^-Na^+$	H	H

The fluorescence studies demonstrate the importance of a cavity as binding site, since with model compound **14c** no binding of TNS was observed under the experimental conditions. The cavity of the smallest host **1c** seems too small to effectively accommodate one of the apolar moieties of TNS. The binding constant of the 1:1 complex between TNS and **2c** is the same as K_a for the 1:1 complex formed between β-cyclodextrin (β-CD) and TNS[34], whereas **3c** and **4c** form stronger complexes than β-CD. On the basis of the fluorescence data it cannot be decided whether in the 1:1 complexes of **2c**–**4c** the naphthalene or the toluene moiety of **30** is preferably enclosed in the cavity. CPK molecular models indicate that both moieties cannot be accommodated in the cavity of even the largest host **4c**.

Complexation studies with ethyl anthranilate (**31**) evidenced that the cavity of **2c** but not of **1c** can incorporate a benzene guest. The fluorescence emission of this guest did not change in aqueous solutions of **1c**. An increase of the fluorescence intensity of **31** however occurred upon addition of **2c** and *Benesi-Hildebrand* treatment gave for the 1:1 complex $K_a = 2.0 \cdot 10^2$ $l \cdot mol^{-1}$ (Table 4)[35].

The cavity of **3c** can accommodate a naphthalene guest like 2,7-naphthalenediol (**32b**). Competitive inhibition of the binding of TNS by **32b** and evaluation of the fluorescence of TNS by a *Benesi-Hildebrand* type treatment[2b] gave $K_a = 1.2 \cdot 10^3$ $l \cdot mol^{-1}$ for the 1:1 complex between **3c** and **32b** ([TNS] = $2.09 \cdot 10^{-6}$ mol · l^{-1}, [**3c**] = $1.01-10.1 \cdot 10^{-5}$ mol · l^{-1}, [**32b**] = $1.3 \cdot 10^{-3}$ mol · l^{-1}; T = 292.5 K; λ_{exc} = 360 nm, λ_{em} = 445 nm).

The stepwise introduction of two, four, six, and eight methyl groups at the diphenylmethane units of hosts **5c**–**8c** was expected to lead incrementally to a stronger binding of apolar guests. This could be demonstrated qualitatively by monitoring the fluorescence of TNS in aqueous solutions of these compounds.

Table 4. Association constants K_a (l · mol^{-1}, 292.5 K) of 1:1 complexes obtained from *Benesi-Hildebrand* evaluation of fluorescence titrations

Host	Guest	K_a (l · mol^{-1})	Experimental Conditions [H_0] (mol · l^{-1})[a]	[G_0] (mol · l^{-1})[a]	λ_{exc} (nm)	λ_{em} (nm)
2c	**30**	$1.5 \cdot 10^3$	$5.1 \cdot 10^{-4} - 5.1 \cdot 10^{-5}$	$2.5 \cdot 10^{-6}$	360	445
3c	**30**	$4.3 \cdot 10^3$	$1.0 \cdot 10^{-4} - 1.0 \cdot 10^{-5}$	$1.2 \cdot 10^{-6}$	360	447
4c	**30**	$1.1 \cdot 10^4$	$1.0 \cdot 10^{-4} - 1.0 \cdot 10.^{-5}$	$1.1 \cdot 10^{-6}$	360	454
2c	**31**	$2.0 \cdot 10^2$	$2.1 \cdot 10^{-3} - 2.1 \cdot 10^{-4}$	$2.9 \cdot 10^{-5}$	360	413

[a] [H_0], [G_0] = total (initial) concentrations of host and guest.

Table 5. Δδ-values (ppm) of the protons of the guests **33a–l** in a D_2O-solution of host **2c** (360 MHz, 303 K, TSP ext; [H_0] = [G_0] = $1 \cdot 10^{-3}$ mol · l^{-1})

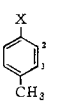

33a-l

X	**33a** H	**33b** CH_3	**33c** CH_2OH	**33d** OH	**33e** CH_2CO_2H	**33f** CH_2NH_2	**33g** Br	**33h** CO_2H	**33i** SO_3^-	**33j** SO_2NH_2	**33k** NO_2	**33l** CN
2-H	+0.02	+0.07	+0.02	+0.02	+0.09	+0.19	+0.15	+0.09	+0.10	+0.08	+0.48	+0.58
3-H				+0.06		+0.12	+0.18	+0.22	+0.39	+0.26	+0.37	+0.30
CH_2			+0.02		+0.04	+0.24						
CH_3	+0.12	+0.07	+0.07	+0.08	+0.11	+0.10	+0.16	+0.20	+0.36	+0.21	+0.22	+0.20

Figure 3 shows that the increase of the fluorescence intensity of TNS ($[H_0] = [G_0] = 1 \cdot 10^{-5}$ mol $\cdot$ l^{-1}) follows as expected the sequence **5c** → **6c** → **7c** → **8c**. A quantitative evaluation of the binding ability of these hosts was not attempted, since the low CMCs prevented the application of the experimental condition $[H_0] \gg [G_0]$ in the *Benesi-Hildebrand* treatment[36]. The qualitative observations were useful inasmuch as they led to the introduction of the methyl groups in host **29**.

^{1}H NMR Studies. The question, how large a guest can be and still fit into the cavity of a particular host, could be answered by the fluorescence studies only for the smallest macrocycle **1c**. A benzene ring seems already too large to be enclosed into the cavity of this host. By ^{1}H NMR we hoped to answer this question also for the larger hosts. Furthermore, we expected from NMR studies informations about the geometry of the complexes. **1c**–**8c** are suitable hosts for NMR studies of complexation, since the anisotropy of the aromatic cavity walls specifically influences the chemical shifts of those protons of complexed guests which are located within the cavity. The low CMC-values, especially of the larger hosts, however, are not favourable for NMR investigations of host-guest complexation. If the exchange between free and complexed host and/or between free and complexed guest is fast on the NMR time scale, the signals of both components appear at the average of the chemical shifts of free and complexed host and/or of free and complexed guest. Averaged signals were observed in all studies described below. At very low concentrations ($[H_0] = [G_0] \leqslant 10^{-4}$ mol $\cdot$ l^{-1}) with K_a-values in the range of those shown in Table 4, only a small amount of host and guest in the solution is complexed. Under these circumstances, the averaged signals in the solution of the complex are only weakly shifted compared to the signals from solutions of pure host and guest and only limited information can be obtained about the structure of the complex in solution.

We looked at the complementarity of aromatic guests of different size to the cavities of **1c**–**3c**. In agreement with the fluorescence studies no complexation was observed by NMR with **14c**. In D_2O-solutions of **14c** and aromatic guests ($[H_0] = [G_0] = 1 \cdot 10^{-3}$ mol $\cdot$ l^{-1}), the signals of both components appeared at exactly the same positions ($\Delta\delta = \pm 0.01$ ppm, 360 MHz, 303 K, TSP ext.) as in the solution of the pure components. In D_2O-solutions ($[H_0] = [G_0] = 1 \cdot 10^{-3}$ mol $\cdot$ l^{-1}) of the smallest macrocycle **1c** and *p*-tolylacetic acid (**33e**) or *p*-toluenesulfonate (**33i**), small upfield shifts of protons of the guest were observed [**33e**: $\Delta\delta$[37] = +0.03 (CH_3); **33i**: $\Delta\delta$ = +0.02 (2-H), +0.10 (3-H), +0.14 (CH_3)]. The comparison with the $\Delta\delta$-values observed for these guests in solutions of the larger host **2c** (Table 5) indicates weak complexation with only the methyl groups of the two guests entering the shielding cavity of **1c**. Thus, in agreement with the fluorescence studies, the NMR data suggest that a benzene ring does not fit completely into the cavity of **1c**.

The ^{1}H NMR data of Table 5 clearly demonstrate the complementarity of the cavity of **2c** to the size of benzene guests. Naphthalene guests like 2,6- and 2,7-naphthalenediol (**32a**, **32b**) or 2-naphthalenesulfonate (**32c**) however cannot be

accommodated in the cavity of **2c**. No changes of the chemical shifts were observed for all protons of these guests in solutions of **2c** with $[H_0] = [G_0] = 1 \cdot 10^{-3}$ mol $\cdot$ l^{-1}. We therefore can conclude that in the 1:1 complex of **2c** and TNS the toluene moiety of the guest is enclosed in the cavity of the host. Naphthalene and substituted derivatives **32a–c** can be incorporated into the cavity of **3c**. Upfield shifts are observed for the protons of these guests in solutions of **3c** ($[H_0] = [G_0] = 1 \cdot 10^{-4}$ mol $\cdot$ l^{-1})[1]. For the reasons discussed above, the observed $\Delta\delta$-values in this low concentration range are small [naphthalene: $\Delta\delta = +0.05$ (1-H), $+0.02$ (2-H); **32a**: $\Delta\delta = +0.04$ (1-H), $+0.02$ (3-H), $+0.07$ (4-H); **32c**: $\Delta\delta = +0.25$ (1-H), $\approx +0.1$ to $+0.5$ (3,4,5,6,7,8-H)[38]]. The anionic guest **32c**, according to these data, seems to form a considerably stronger complex with **3c** than **32a** and **32b**.

According to the observations at CPK molecular models, the *para*-substituted toluenes **33a–l** can only be located axially within the cavity of **2c**. In this position, the axis of the guest through the methyl group and the substituent is about perpendicular to the mean molecular plane of **2c**. The absence of significant changes in the chemical shifts of the protons of **2c** upon complexation indicates that there is no specific plane in the cavity of **2c** in which the axially enclosed guest is preferably located. Specific changes of the chemical shifts however are observed for the protons of **3c** in the solution of **32c** ($[H_0] = [G_0] = 1 \cdot 10^{-4}$ mol $\cdot$ l^{-1}; $\Delta\delta = +0.14$ (3-H), -0.03 (3′-H), ± 0.00 (N^+-CH_3), ± 0.00 (2′-H), $+0.16$ (2-H), $+0.04$ (8-H), -0.04 (9-H); cf. formula **3c** in Figure 2 for numbering of atoms). The observed up- and downfield shifts upon complexation of the protons of **3c** suggest that at least this naphthalene guest is preferably located in the cavity within the plane passing through the two spiro-carbon atoms perpendicular to the mean plane of **3c**. Protons of **3c** in the direction of this plane are shifted downfield, protons about perpendicular to this plane are shifted upfield. This geometry of complex has been clearly shown for all complexes of **29** with aromatic guests[2c] and also for a complex formed between **32b** and a protonated tetraaza[6.1.6.1]paracyclophane[15b].

CPK molecular models have been most valuable tools in the design of our hosts[1–3]. However, a tight fit observed at the models between the guest and the cavity of the host does not seem favourable for the complexation of apolar hosts and guests in aqueous solution. According to our model examinations, benzene guests should tightly fit into the cavity of **1c** and axially orientated naphthalene guests into the cavity of **2c**. In both cases however, significant complexation was not observed. Based on our experimental results, we suggest that binding cavities for apolar host-guest complexation in aqueous solution have to be designed somewhat larger than suggested by the examination of CPK molecular models.

We studied the complexation between host **2c** and a series of *p*-substituted toluenes (Table 5) in order to obtain informations about the driving forces of complexation. With the same concentrations ($[H_0] = [G_0] = 1 \cdot 10^{-3}$ mol $\cdot$ l^{-1}) and under the assumption of the same axial orientation of all twelve guests in the cavity, the extent of $\Delta\delta$ of the protons of the guest could be expected to be a relative measure of the degree and strength of complexation in this series. Table 5 gives the observed changes of the chemical shifts of the protons of the guest.

Less polar guests like toluene (**33a**), *p*-xylene (**33b**) or *p*-methylbenzyl alcohol (**33c**) exhibit small Δδ-values whereas the protons of polar guests like *p*-nitrotoluene (**33k**) or *p*-methylbenzonitrile (**33l**) show considerable upfield shifts upon complexation.

Being aware of the crudeness of the assumption of similar geometry for all complexes and of the contribution of other effects to be discussed below, we believe that the data of Table 5 show that van der Waals interactions contribute considerably to the binding forces in complexes of our hosts. Aromatic guests with a large molecular dipole are more strongly complexed by **2c** than less polar guests. The association constants of the complexes and their temperature dependency need still to be determined in order to obtain a more quantitative view on the influence of the molecular dipole of a guest on the free binding energy.

In the solutions of **2c** and *p*-nitrotoluene (**33k**) and *p*-methylbenzonitrile (**33l**) the largest Δδ-values are observed for the aromatic protons *ortho* to the polar substituents. The polar substituents of these two guest molecules seem to penetrate deeper into the cavity than the methyl groups.

There are certainly other effects that are contributing to the observed Δδ-values of Table 5. Polar substituents have been shown to lead to the formation of more structured complexes than nonpolar substituents if the cavity of the host has a pronounced apolar character[2c]. The structuring influence results from the higher affinity of the polar groups to the aqueous solution than to the apolar cavity walls. Larger Δδ-values have been observed for protons of the guest in the more structured complexes than in the less structured ones. The association constants of both types of complexes can however be very similar[2c]. That the different Δδ-values of Table 5 result mainly from differences in the strength of complexation and less from the structuring influence of polar groups is demonstrated by the NMR data of a solution of **2c** and 1,4-benzenedimethanol ($[H_0] = [G_0] = 1 \cdot 10^{-3}$ mol $\cdot$ l^{-1}). For both signals of the guest a Δδ-value of only +0.02 ppm is measured, indicating very weak complexation.

Another important aspect in the discussion of the NMR data of Table 5 might be the influence of ionic or polar, non-ionic substituents on the water-structure around the free guest. It has been suggested that ions and molecules such as urea alter hydrophobic interactions in their solutions as consequence of their significant influence on the structure of water[39]. It has been proposed that the disruption of water-structure by structure-breaking (chaotropic) ions reduces the strength of hydrophobic interactions and the tendency of aggregation of apolar solutes[39a]. Structure-making ions on the other hand should lead to enhanced hydrophobic interactions. Little is known about structure-making and structure-breaking properties of ionic or polar, non-ionic functional groups attached to an apolar guest. However, one can assume that such properties have to be considered in the discussion of binding forces in aqueous solution. The large difference in complexation which is observed with aromatic guests bearing different ionic residues might well be related to such properties. As was shown above, efficient complexation occurs between **2c** and *p*-toluenesulfonate and between **3c** and 2-naphthalenesulfonate.

On the contrary, no complexation ($\Delta\delta = \pm 0.00$) was observed between **2c** and benzyltrimethylammonium bromide ($[H_0] = [G_0] = 1 \cdot 10^{-3}$ mol $\cdot$ l^{-1}).

We thank Prof. Dr. *H. A. Staab* for most valuable discussions and for the generous support of this work. We thank Mr. *G. Riethmüller* for the elemental analyses and for his help in preparing the samples for complexation studies.

Experimental Part

Instrumentation and Chemicals. ^{1}H NMR spectra: Bruker WP 80 and HX 360 spectrometer. All δ-values (ppm) in organic solvents refer to TMS as internal standard. All δ-valucs of spectra in D_2O refer to TSP in D_2O as external standard placed in a capillary tube inside the NMR tube. If not stated otherwise, the spectra were recorded at 303 K. In temperature dependent NMR experiments, temperatures were measured with methanol below 310 K and with ethylene glycol above 310 K using published equations[40]. – Mass spectra: Dupont CEC 21-492 instrument (EI, 70 eV). – Uncorrected fluorescence spectra were measured at 292.5 ± 0.1 K with a SLM 8000 spectrofluorometer. Light scattering at 90° was also monitored with this instrument. Aqueous solutions in all experiments were prepared with doubly distilled water from a Heraeus-Schott Bi 4 double distillation apparatus. – Melting points (uncorrected): Büchi (Dr. Tottoli). – Elemental analysis: Carlo Erba Elemental Analyzer 1106, Max-Planck-Institut für medizinische Forschung, Heidelberg.

Dimethylformamide was distilled from calcium hydride prior to use. *p*-Xylene was purified via filtration through neutral alumina. 2,6- and 2,7-naphthalenediol and 1,4-benzenedimethanol were recrystallized from water. 4-Methylbenzyl alcohol, *p*-tolylacetic acid, 4-methylbenzoic acid, *p*-nitrotoluene, and *p*-toluenesulfonamide were recrystallized from ethanol. **23**[18,19] and **25**[18,20] were prepared according to published procedures. **27**, *N*-acetyl-4-piperidone and all other commercially available chemicals for synthesis and complexation studies were of analytical grade, if possible, and were used without further purification.

Complexation Studies. Samples for fluorescence titrations were prepared as described in ref.[2b]. For the NMR studies a $1.8 \cdot 10^{-4}$ M solution of naphthalene in D_2O was prepared by solid-liquid extraction as described in ref.[2b]. Addition of the calculated amount of water gave the desired $1.0 \cdot 10^{-4}$ M D_2O-solution of naphthalene. A $4.3 \cdot 10^{-3}$ M solution of toluene and a $1.1 \cdot 10^{-3}$ M solution of *p*-xylene in D_2O were prepared by shaking the organic solvent with D_2O in a separatory funnel for 10 min. The D_2O-layer was carefully let out after the two phases had separated overnight. Addition of the calculated amounts of D_2O gave the $1.0 \cdot 10^{-3}$ M solutions of both guests which were used in the NMR studies. All other host-guest solutions for NMR were prepared by dissolving the calculated amounts of host and guest in D_2O.

In the section "host-guest complexation in aqueous solution", only changes of the chemical shifts ($\Delta\delta$) upon complexation are given. The NMR Data of pure guests in D_2O (360 MHz; TSP ext.; 303 K), not included in ref.[2c], are given below. These data, often significantly different from the data in organic solvents, are useful for the evaluation of complexation shifts ($\Delta\delta$) in future studies. Except for naphthalene, all concentrations of guest are $1.0 \cdot 10^{-3}$ mol $\cdot$ l^{-1}. Multiplet centers (mc) are given for better comparison. Naphthalene ($c = 1 \cdot 10^{-4}$ mol $\cdot$ l^{-1}): δ = 7.99 (mc; 1-H), 7.60 (mc; 2-H). 1,4-Benzenedimethanol: δ = 7.42 (s; H_{arom}), 4.65 (s; CH_2). Benzyltrimethylammonium bromide: δ = 7.57 (mc; H_{arom}), 4.51 (s; CH_2), 3.11 (s; CH_3). **33a**: δ = 7.32 (mc; H_{arom}), 2.36 (s; CH_3). **33b**: δ = 7.19 (s; H_{arom}), 2.31 (s; CH_3). **33c**: δ = 7.31 (mc; H_{arom}), 4.61 (s; CH_2), 2.35 (s; CH_3). **33d**: δ = 7.15 ("d", J = 8.1 Hz; 3-H), 6.84 ("d", J = 8.1 Hz; 2-H), 2.27 (s; CH_3). **33e**: δ = 7.25 (s; H_{arom}), 3.68 (s; CH_2),

2.34 (s; CH_3). **33f**: δ = 7.29 (s, br; H_{arom}), 3.84 (s; CH_2), 2.35 (s; CH_3). **33g**: δ = 7.49 ("d", *J* = 8.3 Hz; 2-H), 7.19 ("d", *J* = 8.3 Hz; 3-H), 2.31 (s; CH_3). **33h**: δ = 7.92 ("d", *J* = 7.9 Hz; 2-H), 7.38 ("d", *J* = 7.9 Hz; 3-H), 2.43 (s; CH_3). **33j**: δ = 7.82 ("d", *J* = 6.7 Hz; 2-H), 7.47 ("d", *J* = 6.7 Hz; 3-H), 2.45 (s; CH_3). **33k**: δ = 8.17 ("d", *J* = 8.0 Hz; 2-H), 7.46 ("d", *J* = 8.0 Hz; 3-H), 2.48 (s; CH_3). **33l**: δ = 7.69 ("d", *J* = 8 Hz; 2-H), 7.41 ("d", *J* = 8 Hz; 3-H), 2.44 (s; CH_3) (cf. formula **33** for numbering of atoms of **33a–l**).

General Procedure for the Preparation of the Bisphenols **9a–c**: 68.5 g (0.485 mol) of *N*-acetyl-4-piperidone was added to a suspension of 1 mol of phenol in 40 ml of water in a 2-l beaker (94.1 g of phenol for **9a**, 108.1 g of *o*-cresol for **9b**, 122.1 g of 2,6-dimethylphenol for **9c**). The mixture was cooled with an ice bath, and 180 g (1.8 mol) of concentrated sulfuric acid was added portion-wise with stirring so that the reaction temperature did not exceed room temperature. The precipitated products **9b** and **9c** were worked up after standing of the reaction mixture at room temperature for 1 d. The oily viscous reaction mixture of **9a** was let stand for 3 d before work up. The reaction mixture of **9a–c** was dissolved in 1 l of hot acetone/methanol (7:3) and the resulting solution in a 5-l beaker was neutralized by addition of 1 N Na_2CO_3. After addition of water to give a total volume of 4 l, the product precipitated. After cooling, colourless **9a–c** were isolated by filtration, washed several times with water and dried at 120°C in vacuo. **9a–c** thus obtained were of very high purity (TLC, NMR) and were further recrystallized for elemental analysis only (see Table 6 for yields and analytical data).

General Procedure for the Preparation of the Dichlorides **10a–f**, **24**, **26a–c**, *and* **28**: A stirred solution of 0.1 mol of bisphenol (**9a–c**, **23**, **25** or **27**) and 10 g (0.25 mol) of sodium hydroxide in 1 l of *n*-butanol was heated to reflux under N_2. After 1 h, water was added drop-wise to the boiling mixture to give a clear solution. 2 Mol of the corresponding α,ω-dichloroalkane (198 g of 1,2-dichloroethane, 226 g of 1,3-dichloropropane, 254 g of 1,4-dichlorobutane, and 282 g of 1,5-dichloropentane, respectively) in 350 ml of *n*-butanol and 60 g of potassium carbonate were added and the reaction mixture was refluxed for 2 d. The solvents were removed in vacuo and the residue was partitioned between dichloromethane and water. The organic phase was extracted three times with 2 N KOH, washed three times with water and dried over magnesium sulfate. The solvent was removed and chromatography on silica from ethyl acetate yielded the pure products (see Table 6 for yields and analytical data).

General Procedure for the Cyclization to the Tetraoxa[n.1.n.1]paracyclophanes

Method A. Preparation of **11a–h** *and* **18–22**: A stirred mixture of 30 mmol of bisphenol (**9a–c**, **23**, **25** or **27**; see Table 7) and of 2.72 g (68 mmol) of sodium hydroxide in 1.5 l of *n*-butanol was heated to reflux under N_2. After 1 h, 30 mmol of dichloride (**10a–f**, **24**, **26a–c** or **28**; see Table 7) in 1 l of *n*-butanol was added and the resulting mixture was refluxed for 6 d. After neutralization of the solution with glacial acetic acid, the solvent was evaporated under reduced pressure. The residue was partitioned between chloroform and water. The organic layer was extracted three times with 2 N NaOH, washed three times with water, dried over magnesium sulfate and evaporated under reduced pressure. Chromatography on silica from dichloromethane/methanol (10:0.2) followed by recrystallization yielded the pure macrocyclic products (see Table 7 for yields and analytical data).

Method B. Preparation of **11a–h**: 20 mmol of bisphenol (**9a–c**; see Table 7) and 7.82 g (24 mmol) of cesium carbonate in 400 ml of dry methanol were heated to give a clear solution. After complete evaporation of methanol under reduced pressure, 800 ml of dry dimethylformamide was added to the solid residue. From the so obtained solution, 100 ml

of dimethylformamide was distilled off to remove residual traces of methanol and water. 20 mmol of dichloride (**10a–h**; see Table 7) in 1 l of dry dimethylformamide was added to the remaining solution and the resulting mixture was stirred at 60°C for 8 d under N_2. The solvent was removed under reduced pressure and the remaining residue was partitioned between chloroform and water. The organic layer was washed with water, dried over magnesium sulfate, and evaporated in vacuo. Chromatography on silica from dichloromethane/methanol (10:0.2) followed by recrystallization yielded **11a–h** (see Table 7 for yields and analytical data).

General Procedure for the Preparation of the Macrocyclic Bis(spiropiperidines) **12a–h**: 4.0 mmol of **11a–h** and 5.0 g (90 mmol) of potassium hydroxide in 100 ml of 2-methoxyethanol were heated under reflux for 5 h. 40 ml of the solvent was then distilled off and upon drop-wise addition of 50 ml of water to the remaining warm solution, the product precipitated. After standing overnight in the refrigerator, **12a–h** were collected by filtration, washed several times with water, dried in vacuo at 100°C, and recrystallized (see Table 8 for yields and analytical data).

General Procedure for the Eschweiler-Clarke Methylation to **13a–h**: A stirred mixture of 5.0 mmol of **12a–h**, of 2.3 g (50 mmol) of formic acid (98–100%) and of 2.14 g (25 mmol) of a 35% aqueous solution of formaldehyde in a 10-ml flask was heated slowly until the evolution of CO_2 started (at ≈60°C). Stirring was continued without further heating until the end of the evolution of gas; then the mixture was heated to 100°C for 14 h. The reaction mixture was added to 250 ml of 2 N NaOH and the resulting solution was stirred for 1 h at ≈80°C. After standing in the refrigerator, the precipitated crude product was collected by filtration, washed several times with water, and dried in vacuo at 100°C. Chromatography on neutral alumina (Brockmann, activity II–III) from ethyl acetate/chloroform (1:1) followed by recrystallization yielded the pure products **13a–h** (see Table 9 for yields and analytical data).

General Procedure for the Quaternization to the Bis(piperidinium Fluorosulfonates) **1a–8a**: 0.4 mmol of **13a–h** was dissolved in 50 ml of dry chloroform and 275 mg (0.194 ml, 2.4 mmol) of methyl fluorosulfonate was added via syringe. After stirring the mixture under N_2 at room temperature for 14 h, 50 ml of dry ether was added. Stirring was continued for 15 min and after standing for 2 h, the precipitated product was collected by filtration and washed twice with dry ethyl acetate. Recrystallization from methanol/ether followed by drying at 130°C/10^{-3} Torr gave **1a–8a** as hygroscopic colourless solids. For elemental analysis the crystals of **4a–8a** were exposed to laboratory air for 1 h (see Table 10 for yields and analytical data).

General Procedure for the Preparation of the Bis(piperidinium Tetrafluoroborates) **1b–8b**: 0.3 mmol of **1a–8a** was dissolved in 15 ml of water/methanol and 20 ml of an aqueous solution of sodium tetrafluoroborate, saturated at 100°C, was added. After cooling in the refrigerator, the precipitated salt was collected by filtration, washed once with water and dried in vacuo at 100°C. Recrystallization from acetonitrile/ethanol and drying at 170°C/10^{-3} Torr afforded **1b–8b** (see Table 10 for yields and analytical data).

General Procedure for the Preparation of the Bis(piperidinium Chlorides) **1c–8c**: 0.2 mmol of **1a–8a** was chromatographed on ion exchange resin Dowex 1X8 (Cl^-, 200–400 mesh) from water. Recrystallization from methanol/ether followed by drying at 100°C/10^{-3} Torr gave **1c–8c**, which for elemental analysis were exposed to laboratory air for 1 h (see Table 10 for yields and analytical data).

Table 6. Synthetic and analytical data of the cyclization precursors **9a–c**, **10a–f**, **24**, **26a–c** and **28**

Compound	Name of compound	Yield [%]	M.p. [°C]	Formula (mol. wt.)	M^+ (MS)	Elemental analysis	C	H	Cl	N
9a	*N*-Acetyl-4,4-bis(4-hydroxyphenyl)piperidine	76	301 ($PhNO_2$/EtOH)	$C_{19}H_{21}NO_3$ (311.4)	311	Calcd.	73.29	6.80		4.50
						Found	73.09	7.10		4.29
9b	*N*-Acetyl-4,4-bis(4-hydroxy-3-methylphenyl)-piperidine	80	276–278 (Tol./acetone)	$C_{21}H_{25}NO_3$ (339.4)	339	Calcd.	74.31	7.42		4.13
						Found	74.08	7.48		4.00
9c	*N*-Acetyl-4,4-bis(4-hydroxy-3,5-dimethyl-phenyl)piperidine	79	246 (Tol./acetone)	$C_{23}H_{29}NO_3$ (367.5)	367	Calcd.	75.17	7.95		3.81
						Found	75.40	8.10		3.81
10a	*N*-Acetyl-4,4-bis[4-(2-chloroethoxy)phenyl]-piperidine	82	89 (Tol./*n*-hexane)	$C_{23}H_{27}Cl_2NO_3$ (436.4)	435	Calcd.	63.30	6.24	16.25	3.21
						Found	63.56	6.30	16.04	2.98
10b	*N*-Acetyl-4,4-bis[4-(3-chloropropoxy)phenyl]-piperidine	79	87–88 (Tol./*n*-hexane)	$C_{25}H_{31}Cl_2NO_3$ (464.4)	463	Calcd.	64.65	6.73	15.27	3.02
						Found	64.67	6.64	15.31	2.75
10c	*N*-Acetyl-4,4-bis[4-(4-chlorobutoxy)phenyl]-piperidine	88	86–87 (Tol./*n*-hexane)	$C_{27}H_{35}Cl_2NO_3$ (492.5)	491	Calcd.	65.85	7.16	14.40	2.84
						Found	66.14	7.37	14.26	2.83
10d	*N*-Acetyl-4,4-bis[4-(5-chloropentoxy)-phenyl]piperidine	72	Glass	$C_{29}H_{39}Cl_2NO_3$ (520.6)	519	Molecular mass: calcd. 519.2307; found: 519.2304 (M^+, MS)				
10e	*N*-Acetyl-4,4-bis[4-(4-chlorobutoxy)-3-methylphenyl]piperidine	76	96 (Et_2O/*n*-hexane)	$C_{29}H_{39}Cl_2NO_3$ (520.6)	519	Calcd.	66.91	7.55	13.62	2.69
						Found	67.14	7.77	13.77	2.70
10f	*N*-Acetyl-4,4-bis[4-(4-chlorobutoxy)-3,5-dimethylphenyl]piperidine	81	142 (Ethyl acetate)	$C_{31}H_{43}Cl_2NO_3$ (548.6)	547	Calcd.	67.87	7.90	12.93	2.55
						Found	67.97	7.90	13.14	2.46
24	2,2-Bis[4-(4-chlorobutoxy)-3-methylphenyl]-propane	62	Oil $n_D^{20} = 1.5522$	$C_{25}H_{34}Cl_2O_2$ (437.5)	436	Molecular mass: calcd. 436.1936; found: 436.1931 (M^+, MS)				
26a	1,1-Bis[4-(2-chloroethoxy)phenyl]cyclohexane	68	65 (Et_2O/*n*-hexane)	$C_{22}H_{26}Cl_2O_2$ (393.4)	392	Calcd.	67.18	6.66	18.02	
						Found	67.29	7.03	17.85	
26b	1,1-Bis[4-(3-chloropropoxy)phenyl]cyclo-hexane	69	68 (Et_2O/*n*-hexane)	$C_{24}H_{30}Cl_2O_2$ (421.4)	420	Calcd.	68.40	7.18	16.83	
						Found	68.32	6.95	16.55	
26c	1,1-Bis[4-(4-chlorobutoxy)phenyl]cyclo-hexane	71	29 (Et_2O/*n*-hexane)	$C_{26}H_{34}Cl_2O_2$ (449.5)	448	Calcd.	69.48	7.62	15.78	
						Found	69.58	7.74	15.90	
28	Bis[4-(3-chloropropoxy)phenyl]methane	64	45 (*n*-Hexane)	$C_{19}H_{22}Cl_2O_2$ (353.3)	352	Calcd.	64.59	6.28	20.07	
						Found	64.47	6.31	20.29	

Table 6 (*continued*). ^{1}H NMR spectra [80 MHz, δ (ppm), TMS int., *J* (Hz)]

9a	([D$_6$]DMSO):	δ = 1.96 (s; 3H), 2.0–2.35 (m; 4H), 3.2–3.55 (m; 4H), 6.66 and 7.06 (mc, AA′BB′; 8H), 8.92 (s; 2H).
9b	([D$_6$]DMSO):	δ = 1.96 (s; 3H), 2.07 (s; 6H), 2.0–2.35 (m; 4H), 3.2–3.55 (m; 4H), 6.6–7.15 (m; 6H), 8.81 (s, br; 2H).
9c	([D$_6$]DMSO):	δ = 1.95 (s; 3H), 2.10 (s; 12H), 2.0–2.35 (m; 4H), 3.2–3.55 (m; 4H), 6.79 (s; 4H), 7.94 (s; 2H).
10a	(CDCl$_3$):	δ = 2.08 (s; 3H), 2.15–2.45 (m; 4H), 3.35–3.75 (m; 4H), 3.78 („t", *J* = 5.5; 4H), 4.19 („t", *J* = 5.5; 4H), 6.83 and 7.14 (mc, AA′BB′; 8H).
10b	(CDCl$_3$):	δ = 2.07 (s; 3H), 2.20 (t, *J* = 7.6; 4H), 2.2–2.5 (m; 4H), 3.35–3.75 (m; 4H), 3.72 (t, *J* = 7.9; 4H), 4.07 (t, *J* = 7.3; 4H), 6.82 and 7.13 (mc, AA′BB′; 8H).
10c	(CDCl$_3$):	δ = 1.8–2.0 (m; 8H), 2.07 (s; 3H), 2.1–2.4 (m; 4H), 3.35–3.75 (m; 8H), 3.75–4.05 (m; 4H), 6.80 and 7.13 (mc, AA′BB′; 8H).
10d	(CDCl$_3$):	δ = 1.3–2.0 (m; 12H), 2.07 (s; 3H), 2.1–2.4 (m; 4H), 3.35–3.75 (m; 4H), 3.53 („t", *J* ≈ 6.2; 4H), 3.92 („t", *J* ≈ 6.0; 4H), 6.79 and 7.12 (mc, AA′BB′; 8H).
10e	(CDCl$_3$):	δ = 1.75–2.0 (m; 8H), 2.07 (s; 3H), 2.17 (s; 6H), 2.1–2.4 (m; 4H), 3.35–3.75 (m; 8H), 3.8–4.05 (m; 4H), 6.6–7.1 (m; 6H).
10f	(CDCl$_3$):	δ = 1.75–2.05 (m; 8H), 2.07 (s; 3H), 2.21 (s; 12H), 2.1–2.4 (m; 4H), 3.35–3.75 (m; 4H), 3.63 (t, *J* = 8.2; 4H), 3.72 (t, *J* = 6.4; 4H), 6.83 (s; 4H).
24	(CDCl$_3$):	δ = 1.61 (s; 6H), 1.8–2.05 (m; 8H), 2.15 (s; 6H), 3.5–3.75 (m; 4H), 3.8–4.05 (m; 4H), 6.6–7.1 (m; 6H).
26a	(CDCl$_3$):	δ = 1.35–1.7 (m; 6H), 2.05–2.35 (m; 4H), 3.77 („t", *J* ≈ 6.3; 4H), 4.19 („t", *J* ≈ 6.3; 4H), 6.80 and 7.17 (mc, AA′BB′; 8H).
26b	(CDCl$_3$):	δ = 1.35–1.7 (m; 6H), 2.05–2.35 (m; 4H), 2.20 (quint, *J* ≈ 6.0; 4H), 3.72 (t, *J* = 6.1; 4H), 4.07 (t, *J* = 5.8; 4H), 6.79 and 7.17 (mc, AA′BB′; 8H).
26c	(CDCl$_3$):	δ = 1.35–1.7 (m; 6H), 1.85–2.0 (m; 8H), 2.05–2.35 (m; 4H), 3.5–3.7 (m; 4H), 3.85–4.05 (m; 4H), 6.77 and 7.16 (mc, AA′BB′; 8H).
28	(CDCl$_3$):	δ = 2.19 (quint, *J* = 6.1; 4H), 3.71 (t, *J* = 6.4; 4H), 3.85 (s; 2H), 4.07 (t, *J* = 5.8; 4H), 6.80 and 7.08 (mc; AA′BB′; 8H).

Table 7. Synthetic and analytical data of **11a–h** and **18–22**

Compound	Name of compound	Cyclization components	Yield [%] (method)	M.p. [°C]	Formula (mol. wt.)	M⁺ (MS)	Elemental analysis	C	H	N
11a	1′,1″-Diacetyldispiro[1,4,18,21-tetraoxa[4.1.4.1]paracyclophane-11,4′:28,4″-bispiperidine]	**9a + 10a**	14 (A) 14 (B)	335–340 (dec.) (DMSO/EtOH)	$C_{40}H_{46}N_2O_6$ (674.8)	674	Calcd. Found	74.75 74.69	6.87 6.89	4.15 4.09
11b	1′,1″-Diacetyldispiro[1,5,19,23-tetraoxa[5.1.5.1]paracyclophane-12,4′:30,4″-bispiperidine]	**9a + 10b**	13 (A) 18 (B)	283–284 (DMF/EtOH)	$C_{44}H_{50}N_2O_6$ (702.9)	702	Calcd. Found	75.19 75.22	7.17 7.01	3.99 4.16
11c	1′,1″-Diacetyldispiro[1,6,20,25-tetraoxa[6.1.6.1]paracyclophane-13,4′:32,4″-bispiperidine]	**9a + 10c**	15 (A) 19 (B)	264–265 (DMSO/EtOH)	$C_{46}H_{54}N_2O_6$ (730.9)	730	Calcd. Found	75.59 75.53	7.45 7.58	3.83 3.54
11d	1′,1″-Diacetyldispiro[1,7,21,27-tetraoxa[7.1.7.1]paracyclophane-14,4′:34,4″-bispiperidine]	**9a + 10d**	7 (A) 20 (B)	246 (EtOH/Et_2O)	$C_{48}H_{58}N_2O_6$ (759.0)	758	Calcd. Found	75.96 75.96	7.70 7.63	3.69 3.53
11e	1′,1″-Diacetyl-8,16-dimethyldispiro[1,6,20,25-tetraoxa[6.1.6.1]paracyclophane-13,4′:32,4″-bispiperidine]	**9a + 10e**	15 (A) 16 (B)	248 ($CHCl_3$/EtOH/Et_2O)	$C_{48}H_{58}N_2O_6$ (759.0)	758	Calcd. Found	75.96 75.73	7.70 7.92	3.69 3.77
11f	1′,1″-Diacetyl-8,12,16,18-tetramethyldispiro[1,6,20,25-tetraoxa[6.1.6.1]paracyclophane-13,4′:32,4″-bispiperidine]	**9a + 10f**	11 (A) 20 (B)	278 (EtOH/Et_2O)	$C_{50}H_{62}N_2O_6$ (787.1)	786	Calcd. Found	76.30 76.09	7.94 8.04	3.56 3.57
11g	1′,1″-Diacetyl-8,12,16,18,27,35-hexamethyldispiro[1,6,20,25-tetraoxa[6.1.6.1]paracyclophane-13,4′:32,4″-bispiperidine]	**9c + 10e**	7 (A) 12 (B)	288 (EtOH/Et_2O)	$C_{52}H_{66}N_2O_6$ (815.1)	814	Calcd. Found	76.62 76.65	8.16 8.34	3.44 3.56
11h	1′,1″-Diacetyl-8,12,16,18,27,31,35,37-octamethyldispiro[1,6,20,25-tetraoxa[6.1.6.1]paracyclophane-13,4′:32,4″-bispiperidine]	**9c + 10f**	10 (A) 12 (B)	324 (Et_2O)	$C_{54}H_{70}N_2O_6$ (843.2)	842	Calcd. Found	76.92 77.07	8.37 8.51	3.32 3.35
18	8,13,13,16,27,32,32,35-Octamethyl-1,6,20,25-tetraoxa[6.1.6.1]-paracyclophane	**23 + 24**	16 (A)	179 (Tol./EtOH)	$C_{42}H_{52}O_4$ (620.9)	620	Calcd. Found	81.25 81.22	8.44 8.30	

Table 7 (*continued*)

Compound	Name of compound	Cyclization components	Yield [%] (method)	M.p. [°C]	Formula (mol. wt.)	M^+ (MS)	Elemental analysis	C	H	N
19	Dispiro[1,4,18,21-tetraoxa[4.1.4.1]paracyclophane-11,1′:28,1″-biscyclohexane]	**25** + **26a**	16 (A)	308–310 (Tol.)	$C_{40}H_{44}O_4$ (588.8)	588	Calcd.	81.60	7.53	
							Found	81.75	7.71	
20	Dispiro[1,5,19,23-tetraoxa[5.1.5.1]paracyclophane-12,1′:30,1″-biscyclohexane]	**25** + **26b**	13 (A)	233 (Tol.; lit[20]: 218)	$C_{42}H_{48}O_4$ (616.8)	616	Calcd.	81.78	7.84	
							Found	81.60	7.70	
21	Dispiro[1,6,20,25-tetraoxa[6.1.6.1]paracyclophane-13,1′:32,1″-biscyclohexane]	**25** + **26c**	15 (A)	236–237 (Tol./EtOH)	$C_{44}H_{52}O_4$ (644.9)	644	Calcd.	81.95	8.13	
							Found	81.69	8.33	
22	1,5,19,23-Tetraoxa[5.1.5.1]-paracyclophane	**27** + **28**	15 (A)	277 (Tol.)	$C_{32}H_{32}O_4$ (480.6)	480	Calcd.	79.97	6.71	
							Found	79.85	6.84	

^{1}H NMR spectra [80 MHz, δ (ppm), TMS int., *J* (Hz)]

11a ([D_5]nitrobenzene): δ = 2.0–2.55 (m; 8H), 2.19 (s; 6H), 3.25–3.95 (m; 8H), 4.37 (s; 8H), 6.75 and 7.07 (mc, AA′BB′; 16H).
11b ([D_5]nitrobenzene): δ = 1.95–2.5 (m; 12H), 2.14 (s; 6H), 3.25–3.9 (m; 8H), 4.08 (t, *J* = 5.5; 8H), 6.67 and 7.08 (mc, AA′BB′; 16H).
11c ([D_5]nitrobenzene): δ = 1.75–2.0 (m; 8H), 2.05–2.55 (m; 8H), 2.19 (s; 6H), 3.3–4.05 (m; 16H), 6.74 and 7.21 (mc, AA′BB′; 16H).
11d ($CDCl_3$): δ = 1.5–1.95 (m; 12H), 2.07 (s; 6H), 2.1–2.5 (m; 8H), 3.3–3.8 (m; 8H), 3.92 („t", *J* ≈ 5.0; 8H), 6.73 and 7.07 (mc, AA′BB′; 16H).
11e ([D_6]DMSO): δ = 1.65–2.0 (m; 8H), 1.96 (s; 6H), 2.03 (s; 6H), 2.05–2.35 (m; 8H), 3.25–3.55 (m; 8H), 3.95 („t", *J* ≈ 6.0; 8H), 6.7–7.15 (m; 14H).
11f ($CDCl_3$): δ = 1.75–2.05 (m; 8H), 2.05 (s; 3H), 2.05–2.35 (m; 8H), 2.06 (s; 3H, 2.17 (s; 12H), 3.35–4.1 (m; 16H), 6.73 and 8H), 2.06 (s; 3H), 2.17 (s; 12H), 3.35–4.1 (m; 16H), 6.73 and 7.06 7.06 (mc, AA′BB′; 8H), 6.79 (s; 4H).
11g ($CDCl_3$): δ = 1.75–2.05 (m; 8H), 2.05–2.35 (m; 8H), 2.06 (s; 6H), 2.08 (s; 6H), 2.15 (s; 12H), 3.35–4.1 (m; 16H), 6.55–7.0 (m; 6H), 6.76 (s; 4H).
11h ($CDCl_3$): δ = 1.75–2.05 (m; 8H), 2.05 (s; 6H), 2.05–2.35 (m; 8H), 2.15 (s; 24H), 3.35–3.95 (m; 16H), 6.77 (s; 8H).
18 ($CDCl_3$): δ = 1.60 (s; 12H), 1.85–2.1 (m; 8H), 2.03 (s; 12H), 3.85–4.1 (m; 8H), 6.55–7.05 (m; 12H).
19 ($CDCl_3$): δ = 1.4–1.75 (m; 12H), 2.05–2.35 (m; 8H), 4.26 (s; 8H), 6.70 and 7.04 (mc, AA′BB′; 16H).
20 ($CDCl_3$): δ = 1.35–1.8 (m; 12H), 2.0–2.4 (m; 8H), 2.10 (quint, *J* = 5.2; 4H), 4.00 (t, *J* = 5.2; 8H), 6.70 and 7.09 (mc, AA′BB′; 16H).
21 ($CDCl_3$): δ = 1.35–1.75 (m; 12H), 1.75–2.0 (m; 8H), 2.0–2.35 (m; 8H), 3.75–4.05 (m; 8H), 6.71 and 7.11 (mc, AA′BB′; 16H).
22 ($CDCl_3$): δ = 2.12 (quint, *J* = 5.4; 4H), 3.73 (s; 4H), 4.05 (t, *J* = 5.4; 8H), 6.70 and 7.02 (mc, AA′BB′; 16H).

Table 8. Synthetic and analytical data of **12a–h**

Compound	Name of compound	Yield [%]	M.p. [°C]	Formula (mol. wt.)	M^+ (MS)	Elemental analysis	C	H	N
12a	Dispiro[1,4,18,21-tetraoxa[4.1.4.1]paracyclophane-11,4′:28,4″-bispiperidine]	81	316 (dec.) (Tol.)	$C_{38}H_{42}N_2O_4$ (590.8)	590	Calcd.	77.26	7.17	4.74
						Found	77.42	7.25	4.48
12b	Dispiro[1,5,19,23-tetraoxa[5.1.5.1]paracyclophane-12,4′:30,4″-bispiperidine]	95	243–244 (Tol./EtOH)	$C_{40}H_{46}N_2O_4$ (618.8)	618	Calcd.	77.64	7.49	4.53
						Found	77.61	7.52	4.44
12c	Dispiro[1,6,20,25-tetraoxa[6.1.6.1]paracyclophane-13,4′:32.4″-bispiperidine]	85	266–270 (EtOH)	$C_{42}H_{50}N_2O_4$ (646.9)	646	Calcd.	77.98	7.79	4.33
						Found	78.16	8.02	4.14
12d	Dispiro[1,7,21,27-tetraoxa[7.1.7.1]paracyclophane-14,4′:34,4″-bispiperidine]	85	238–239 (Tol.)	$C_{44}H_{54}N_2O_4$ (674.9)	674	Calcd.	78.30	8.06	4.15
						Found	78.12	8.09	4.11
12e	8,16-Dimethyldispiro[1,6,20,25-tetraoxa[6.1.6.1]paracyclophane-13,4′:32,4″-bispiperidine]	95	213 (EtOH)	$C_{44}H_{54}N_2O_4$ (674.9)	674	Calcd.	78.30	8.06	4.15
						Found	78.14	8.05	4.32
12f	8,12,16,18-Tetramethyldispiro[1,6,20,25-tetraoxa[6.1.6.1]paracyclophane-13,4′:32,4″-bispiperidine]	80	263 (EtOH)	$C_{46}H_{58}N_2O_4$ (703.0)	702	Calcd.	78.59	8.32	3.99
						Found	78.37	8.24	4.15
12g	8,12,16,18,27,35-Hexamethyldispiro[1,6,20,25-tetraoxa[6.1.6.1]paracyclophane-13,4′:32,4″-bispiperidine]	89	273 (EtOH)	$C_{48}H_{62}N_2O_4$ (731.0)	730	Calcd.	78.86	8.55	3.83
						Found	78.88	8.49	4.04
12h	8,12,16,18,27,31,35,37-Octamethyldispiro[1,6,20,25-tetraoxa[6.1.6.1]paracyclophane-13,4′:32,4″-bispiperidine]	89	279 (EtOH)	$C_{50}H_{66}N_2O_4$ (759.1)	758	Calcd.	79.11	8.76	3.69
						Found	79.31	8.77	3.57

Table 8 (*continued*). ^{1}H NMR spectra [80 MHz, $CDCl_3$, δ (ppm), TMS int., *J* (Hz)]

12a: δ = 1.53 (s, br; 2H), 2.1–2.4 (m; 8H), 2.75–3.0 (m; 8H), 4.27 (s; 8H), 6.71 and 7.03 (mc, AA′BB′; 16H).

12b: δ = 1.61 (s, br; 2H), 2.13 (quint, *J* = 6.4; 4H), 2.15–2.5 (m; 8H), 2.7–3.05 (m; 8H), 4.01 (t, *J* = 6.4; 8H), 6.68 and 7.11 (mc, AA′BB′; 16H).

12c: δ = 1.75 (s, br; 2H), 1.75–2.05 (m; 8H), 2.15–2.5 (m; 8H), 2.75–3.1 (m; 8H), 3.75–4.1 (m; 8H), 6.71 and 7.09 (mc, AA′BB′; 16H).

12d: δ = 1.56 (s, br; 2H), 1.5–1.95 (m; 12H), 2.1–2.5 (m; 8H), 2.75–3.05 (m; 8H), 3.75–4.05 (m; 8H), 6.72 and 7.08 (mc, AA′BB′; 16H).

12e: δ = 1.57 (s, br; 2H), 1.8–2.1 (m; 8H), 2.1–2.45 (m; 8H), 2.11 (s; 6H), 2.75–3.05 (m; 8H), 3.75–4.05 (m; 8H), 6.55–7.15 (m; 14H).

12f: δ = 1.63 (s, br; 2H), 1.8–2.1 (m; 8H), 2.1–2.4 (m; 8H), 2.16 (s; 12H), 2.75–3.05 (m; 8H), 3.55–4.1 (m; 8H), 6.72 and 7.08 (mc, AA′BB′; 8H), 6.78 (s; 4H).

12g: δ = 1.55 (s, br; 2H), 1.8–2.1 (m; 8H), 2.09 (s; 6H), 2.1–2.45 (m; 8H), 2.15 (s; 12H), 2.75–3.05 (m; 8H), 3.6–4.1 (m; 8H), 6.55–7.0 (m; 6H), 6.78 (s; 4H).

12h: δ = 1.54 (s, br; 2H), 1.8–2.1 (m; 8H), 2.1–2.4 (m; 8H), 2.15 (s; 24H), 2.7–3.0 (m; 8H), 3.6–3.95 (m; 8H), 6.78 (s; 8H).

Table 9. Synthetic and analytical data of **13a–h**

Compound	Name of compound	Yield [%]	M.p. [°C]	Formula (mol. wt.)	M^+ (MS)	Elemental analysis	C	H	N
13a	1′,1″-Dimethyldispiro[1,4,18,21-tetraoxa[4.1.4.1]paracyclophane-11,4′: 28,4″-bispiperidine]	61	306–307 (Tol./EtOH)	$C_{40}H_{46}N_2O_4$ (618.8)	618	Calcd.	77.64	7.49	4.53
						Found	77.64	7.70	4.51
13b	1′,1″-Dimethyldispiro[1,5,19,23-tetraoxa[5.1.5.1]paracyclophane-12,4′: 30,4″-bispiperidine]	60	238 (Tol./EtOH)	$C_{42}H_{50}N_2O_4$ (646.9)	646	Calcd.	77.98	7.79	4.33
						Found	78.02	7.71	4.40
13c	1′,1″-Dimethyldispiro[1,6,20,25-tetraoxa[6.1.6.1]paracyclophane-13,4′: 32,4″-bispiperidine]	81	219 (Tol./EtOH)	$C_{44}H_{54}N_2O_4$ (674.9)	674	Calcd.	78.30	8.06	4.15
						Found	78.42	8.15	4.07
13d	1′,1″-Dimethyldispiro[1,7,21,27-tetraoxa[7.1.7.1]paracyclophane-14,4′: 34,4″-bispiperidine]	58	212 ($Tol./Et_2O$)	$C_{46}H_{58}N_2O_4$ (703.0)	702	Calcd.	78.59	8.32	3.99
						Found	78.79	8.46	3.77

Table 9 (*continued*)

Compound	Name of compound	Yield [%]	M.p. [°C]	Formula (mol. wt.)	M^+ (MS)	Elemental analysis	C	H	N
13e	1′,1″,8,16-Tetramethyldispiro[1,6,20,25-tetraoxa[6.1.6.1]paracyclophane-13,4′:32,4″-bispiperidine]	70	249 (Tol./EtOH)	$C_{46}H_{58}N_2O_4$ (703.0)	702	Calcd.	78.59	8.32	3.99
						Found	78.78	8.55	4.27
13f	1′,1″,8,12,16,18-Hexamethyldispiro[1,6,20,25-tetraoxa[6.1.6.1]paracyclophane-13,4′:32,4″-bispiperidine]	68	268 (EtOH/Et_2O)	$C_{48}H_{62}N_2O_4$ (731.0)	730	Calcd.	78.86	8.55	3.83
						Found	78.68	8.56	4.12
13g	1′,1″,8,12,16,18,27,35-Octamethyldispiro[1,6,20,25-tetraoxa[6.1.6.1]paracyclophane-13,4′:32,4″-bispiperidine]	79	265 (EtOH/Et_2O)	$C_{50}H_{66}N_2O_4$ (759.1)	758	Calcd.	79.11	8.76	3.69
						Found	79.23	8.77	3.61
13h:	1′,1″,8,12,16,18,27,31,35,37-Decamethyldispiro[1,6,20,25-tetraoxa[6.1.6.1]paracyclophane-13,4′:32,4″-bispiperidine]	75	325 (Tol./EtOH)	$C_{52}H_{70}N_2O_4$ (787.1)	786	Calcd.	79.35	8.96	3.56
						Found	79.52	8.96	3.36

^{1}H NMR spectra [80 MHz, $CDCl_3$, δ (ppm), TMS int., *J* (Hz)]

13a: δ = 2.20 (s; 6H), 2.2–2.6 (m; 16H), 4.27 (s; 8H), 6.70 and 7.02 (mc, AA′BB′; 16H).

13b: δ = 2.10 (quint, *J* = 6.4; 4H), 2.19 (s; 6H), 2.25–2.6 (m; 16H), 4.01 (t, *J* = 6.4; 8H), 6.68 and 7.11 (mc, AA′BB′; 16H).

13c: δ = 1.7–2.0 (m; 8H), 2.1–2.5 (m; 16H), 2.20 (s; 6H), 3.7–4.0 (m; 8H), 6.71 and 7.09 (mc, AA′BB′; 16H).

13d: δ = 1.35–1.95 (m; 12H), 2.1–2.6 (m; 16H), 2.20 (s; 6H), 3.75–4.05 (m; 8H), 6.70 and 7.07 (mc, AA′BB′; 16H).

13e: δ = 1.75–2.05 (m; 8H), 2.10 (s; 6H), 2.1–2.6 (m; 16H), 2.19 (s; 6H), 3.75–4.05 (m; 8H), 6.5–7.1 (m; 14H).

13f: δ = 1.75–2.05 (m; 8H), 2.1–2.6 (m; 16H), 2.16 (s; 12H), 2.19 (s; 6H), 3.6–4.1 (m; 8H), 6.72 and 7.07 (mc, AA′BB′; 8H), 6.78 (s; 4H).

13g: δ = 1.75–2.05 (m; 8H), 2.08 (s; 6H), 2.1–2.6 (m; 16H), 2.15 (s; 12H), 2.19 (s; 6H), 3.6–4.1 (m; 8H), 6.55–7.0 (m; 6H), 6.78 (s; 4H).

13h: δ = 1.75–2.05 (m; 8H), 2.1–2.6 (m; 16H), 2.15 (s; 24H), 2.17 (s; 6H), 3.6–3.95 (m; 8H), 6.77 (s; 8H).

Table 10. Synthetic and analytical data of **1a–8a**, **1b–8b** and **1c–8c**

Compound	Name of compound	Yield [%]	Decompn. temp. (°C)	Formula (mol. wt.)	Elemental analysis	C	H	N		
1a	1′,1′,1″,1″-Tetramethyldispiro[1,4,18,21-tetraoxa[4.1.4.1]paracyclophane-11,4′:28,4″-bis-piperidinium] Bis(fluorosulfonate)	89	>330	$C_{42}H_{52}F_2N_2O_{10}S_2$ (847.0)	Calcd.	59.55	6.19	3.31	S	7.57
					Found	59.78	6.28	3.25	S	7.41
1b	Bis(tetrafluoroborate)	78	>370	$C_{42}H_{52}B_2F_8N_2O_4$ (822.5)	Calcd.	61.33	6.37	3.41	B	2.63
					Found	61.26	6.36	3.24	B	2.50
1c	Dichloride	86	300–304	$C_{42}H_{52}Cl_2N_2O_4 \times 2.5\ H_2O$ (764.8)	Calcd.	65.96	7.51	3.66	Cl	9.27
					Found	65.86	7.67	3.69	Cl	9.22
2a	1′,1′,1″,1″-Tetramethyldispiro(1,5,19,23-tetraoxa[5.1.5.1]paracyclophane-12,4′:30,4″-bis-piperidinium] Bis(fluorosulfonate)	95	299–301	$C_{44}H_{56}F_2N_2O_{10}S_2$ (875.1)	Calcd.	60.39	6.45	3.20	S	7.33
					Found	60.37	6.47	3.12	S	7.37
2b	Bis(tetrafluoroborate)	85	>365	$C_{44}H_{56}B_2F_8N_2O_4$ (850.6)	Calcd.	62.13	6.64	3.29	B	2.54
					Found	62.01	6.90	3.28	B	2.36
2c	Dichloride	84	298–301	$C_{44}H_{56}Cl_2N_2O_4 \times 2\ H_2O$ (783.9)	Calcd.	67.42	7.72	3.57	Cl	9.05
					Found	67.35	7.85	3.56	Cl	9.09
3a	1′,1′,1″,1″-Tetramethyldispiro[1,6,20,25-tetraoxa[6.1.6.1]paracyclophane-13,4′:32,4″-bis-piperidinium] Bis(fluorosulfonate)	90	>275	$C_{46}H_{60}F_2N_2O_{10}S_2$ (903.1)	Calcd.	61.18	6.70	3.10	S	7.10
					Found	61.11	6.79	2.97	S	6.87
3b	Bis(tetrafluoroborate)	64	>360	$C_{46}H_{60}B_2F_8N_2O_4$ (878.6)	Calcd.	62.88	6.88	3.19	B	2.46
					Found	62.87	6.86	3.19	B	2.39
3c	Dichloride	91	229	$C_{46}H_{60}Cl_2N_2O_4 \times 4\ H_2O$ (848.0)	Calcd.	65.15	8.08	3.30	Cl	8.36
					Found	65.37	8.14	3.36	Cl	8.36
4a	1′,1′,1″,1″-Tetramethyldispiro[1,7,21,27-tetraoxa[7.1.7.1]paracyclophane-14,4′:34,4″-bis-piperidinium] Bis(fluorosulfonate)	82	220	$C_{48}H_{64}F_2N_2O_{10}S_2 \times 2\ H_2O$ (967.2)	Calcd.	59.61	7.09	2.90	S	6.63
					Found	59.65	7.24	2.71	S	6.64
4b	Bis(tetrafluoroborate)	75	>335	$C_{48}H_{64}B_2F_8N_2O_4$ (906.7)	Calcd.	63.59	7.12	3.09	B	2.39
					Found	63.40	7.04	3.35	B	2.22
4c	Dichloride	80	>288	$C_{48}H_{64}Cl_2N_2O_4 \times 2\ H_2O$ (840.0)	Calcd.	68.63	8.16	3.34	Cl	8.44
					Found	68.75	8.41	3.25	Cl	8.17

Table 10 (*continued*)

Compound	Name of compound	Yield [%]	Decompn. temp. (°C)	Formula (mol. wt.)	Elemental analysis	C	H	N		
5a	1′,1′,1″,1″,8,16-Hexamethyldispiro[1,6,20,25-tetraoxa[6.1.6.1]paracyclophane-13,4′:32,4″-bis-piperidinium] Bis(fluorosulfonate)	82	284	$C_{48}H_{64}F_2N_2O_{10}S_2 \times 2\ H_2O$ (967.2)	Calcd.	59.61	7.09	2.90	S	6.63
					Found	59.62	7.19	2.67	S	6.79
5b	Bis(tetrafluoroborate)	87	>345	$C_{48}H_{64}B_2F_8N_2O_4$ (906.6)	Calcd.	63.59	7.12	3.09	B	2.38
					Found	63.69	7.41	3.06	B	2.24
5c	Dichloride	79	>320	$C_{48}H_{64}Cl_2N_2O_4 \times 2\ H_2O$ (840.0)	Calcd.	68.63	8.16	3.34	Cl	8.44
					Found	68.75	8.41	3.25	Cl	8.17
6a	1′,1′,1″,1″,8,12,16,18-Octamethyldispiro[1,6,20,25-tetraoxa[6.1.6.1]paracyclophane-13,4′:32,4″-bis-piperidinium] Bis(fluorosulfonate)	85	328	$C_{50}H_{68}F_2N_2O_{10}S_2 \times 2\ H_2O$ (995.3)	Calcd.	60.34	7.29	2.81	S	6.44
					Found	60.38	7.47	2.87	S	6.45
6b	Bis(tetrafluoroborate)	62	>340	$C_{50}H_{68}B_2F_8N_2O_4$ (934.7)	Calcd.	64.25	7.33	3.00	B	2.32
					Found	64.14	7.33	3.00	B	2.14
6c	Dichloride	77	>280	$C_{50}H_{68}Cl_2N_2O_4 \times 3\ H_2O$ (886.1)	Calcd.	67.78	8.42	3.16	Cl	8.00
					Found	67.74	8.12	3.01	Cl	8.28
7a	1′,1′,1″,1″,8,12,16,18,27,35-Decamethyldispiro[1,6,20,25-tetraoxa[6.1.6.1]paracyclophane-13,4′:32,4″-bis-piperidinium] Bis(fluorosulfonate)	82	314	$C_{52}H_{72}F_2N_2O_{10}S_2 \times 3\ H_2O$ (1041.3)	Calcd.	59.98	7.55	2.69	S	6.16
					Found	60.10	7.27	2.79	S	6.50
7b	Bis(tetrafluoroborate)	66	>360	$C_{52}H_{72}B_2F_8N_2O_4$ (962.8)	Calcd.	64.87	7.54	2.91	B	2.25
					Found	65.04	7.66	2.98	B	2.27
7c	Dichloride	88	>305	$C_{52}H_{72}Cl_2N_2O_4 \times 3\ H_2O$ (914.1)	Calcd.	68.33	8.60	3.06	Cl	7.76
					Found	68.19	8.71	3.30	Cl	7.74
8a	1′,1′,1″,1″,8,12,16,18,27,31,35,37-Dodecamethyldispiro[1,6,20,25-tetraoxa[6.1.6.1]paracyclophane-13,4′:32,4″-bis-piperidinium] Bis(fluorosulfonate)	86	>321	$C_{54}H_{76}F_2N_2O_{10}S_2 \times 2\ H_2O$ (1051.4)	Calcd.	61.69	7.67	2.66	S	6.10
					Found	61.62	7.72	2.71	S	6.10
8b	Bis(tetrafluoroborate)	67	>340	$C_{54}H_{76}B_2F_8N_2O_4 \times H_2O$ (1008.9)	Calcd.	64.29	7.79	2.78	B	2.14
					Found	64.07	7.63	2.75	B	2.14
8c	Dichloride	68	303	$C_{54}H_{76}Cl_2N_2O_4 \times 3\ H_2O$ (942.2)	Calcd.	68.84	8.77	2.97	Cl	7.53
					Found	69.12	8.87	3.04	Cl	7.73

Table 10 (*continued*). ^{1}H NMR spectra [δ (ppm), 303 K]

1c	(360 MHz, D_2O, TSP ext.; [**1c**] = $8 \cdot 10^{-4}$ mol·l^{-1}): δ = 2.74 (mc; 8H), 3.13 (s; 12H), 3.42 (mc; 8H), 4.37 (s; 8H), 6.87 and 7.24 (mc, AA′BB′; 16H).
2c	(80 MHz, D_2O, TSP ext.; [**2c**] = $8 \cdot 10^{-4}$ mol·l^{-1}): δ = 2.16 (quint, J = 5.6 Hz; 4H), 2.76 (mc; 8H), 3.11 (s; 12H), 3.39 (mc; 8H), 4.12 (t, J = 5.6 Hz; 8H), 6.86 and 7.24 (mc, AA′BB′; 16H).
3c	(360 MHz, D_2O, TSP ext.; [**3c**] = $1 \cdot 10^{-4}$ mol·l^{-1}): δ = 1.88 (mc; 8H), 2.74 (mc; 8H), 3.15 (s; 12H), 3.43 (mc; 8H), 4.09 (mc; 8H), 6.82 and 7.25 (mc, AA′BB′; 16H).
4c	(80 MHz, [D_4]methanol, TMS int.): δ = 1.35–2.0 (m; 12H), 2.35–2.9 (m; 8H), 2.9–3.35 (m; 8H), 3.02 (s; 12H), 3.65–4.05 (m; 8H), 6.82 and 7.20 (mc, AA′BB′; 16H).
5c	(80 MHz, [D_4]methanol, TMS int.): δ = 1.75–2.15 (m; 8H), 2.04 (s; 6H), 2.5–2.9 (m; 8H), 3.14 (s; 12H), 3.2–3.55 (m; 8H), 3.8–4.15 (m; 8H), 6.7–7.3 (m; 14H).
6c	(80 MHz, [D_4]methanol, TMS int.): δ = 1.75–2.05 (m; 8H), 2.17 (s; 12H), 2.55–2.9 (m; 8H), 3.16 (s; 12H), 3.2–3.55 (m; 8H), 3.6–4.15 (m; 8H), 6.82 and 7.20 (mc, AA′BB′; 8H), 6.93 (s; 4H).
7c	(80 MHz, [D_4]methanol, TMS int.): δ = 1.75–2.05 (m; 8H), 2.05 (s; 6H), 2.16 (s; 12H), 2.5–2.9 (m; 8H), 3.16 (s; 12H), 3.2–3.55 (m; 8H), 3.65–4.2 (m; 8H), 6.7–7.2 (m; 6H), 6.92 (s; 4H).
8c	(80 MHz, [D_4]methanol, TMS int.): δ = 1.75–2.05 (m; 8H), 2.16 (s; 24H), 2.5–2.9 (m; 8H), 3.14 (s; 12H), 3.2–3.55 (m; 8H), 3.55–3.95 (m; 8H), 6.95 (s; 8H).

N-Acetyl-4,4-bis(4-methoxyphenyl)piperidine (**16a**): 100 g (0.125 mol) of a 5% aqueous solution of sodium hydroxide was added under N_2 to 15.55 g (0.05 mol) of **9a** and the mixture was stirred to give a clear solution. 12.61 g (0.1 mol) of dimethyl sulfate was slowly added drop-wise below 40°C and the resulting mixture was heated to 100°C for 30 min. After cooling, the aqueous solution was extracted three times with ether/toluene (1:1). The combined organic layers were washed once with 2 N NaOH, once with water, dried over magnesium sulfate and evaporated in vacuo. Chromatography on silica from ethyl acetate followed by recrystallization from ether/ligroin (40–80°C) afforded 9.9 g (58%) of **16a**, m.p. 92°C. – ^{1}H NMR (80 MHz, $CDCl_3$): δ = 2.08 (s; 3H), 2.15–2.45 (m; 4H), 3.4–3.7 (m; 4H), 3.76 (s; 6H), 6.81 and 7.14 (mc, AA'BB'; 8H). – MS: *m/z* = 339 (M^+).

$C_{21}H_{25}NO_3$ (339.4) Calcd. C 74.31 H 7.42 N 4.13 Found C 74.60 H 7.20 N 4.06

N-Acetyl-4,4-bis(4-methoxy-3,5-dimethylphenyl)piperidine (**16b**): **16b** was prepared from 9.4 g (25.6 mmol) of **9c** according to the procedure described for **16a**. **16b** was obtained as colourless solid after evaporation of the ether/toluene mixture and recrystallization from toluene/ligroin (60–95°C) afforded 9.6 g (95%) of **16b**, m.p. 168–169°C. – ^{1}H NMR (80 MHz, $CDCl_3$): δ = 2.1–2.4 (m; 4H), 2.20 (s; 3H), 2.23 (s; 12H), 3.35–3.65 (m; 4H), 3.68 (s; 6H), 6.83 (s; 4H). – MS: *m/z* = 395 (M^+).

$C_{25}H_{33}NO_3$ (395.5) Calcd. C 75.91 H 8.41 N 3.54 Found C 75.72 H 8.47 N 3.59

4,4-Bis(4-methoxyphenyl)-N-methylpiperidine (**17a**): 3.39 g (10 mmol) of **16a** and 5.6 g (0.1 mol) of potassium hydroxide in 150 ml of 2-methoxyethanol were heated to reflux for 6 h. After evaporation of 100 ml of the solvent in vacuo, 200 ml of water was added. The aqueous solution was extracted four times with ether. The combined organic phases were washed three times with ether, dried over sodium sulfate and evaporated in vacuo to yield 2.5 g of crude 4,4-bis(4-methoxyphenyl)piperidine, which was used in the following Eschweiler-Clarke methylation without further purification. 2.55 g (55.4 mmol) of formic acid (98–100%) and 1.88 g (22 mmol) of 35% aqueous solution of formaldehyde were added and the stirred mixture was heated slowly until the beginning of the evolution of CO_2 (at ≈60°C). Stirring was continued without further heating until the end of the evolution of gas and the solution was then heated to 100°C for 14 h. After cooling, the reaction mixture was added to 150 ml of 2 N NaOH and the aqueous solution was extracted three times with ether. The combined ethereal phases were washed three times with water, dried over sodium sulfate and the ether was distilled off. Chromatography of the residue on neutral alumina (Brockmann, activity II–III) from ethyl acetate followed by recrystallization from ether gave 1.9 g (61%) of **17a**, m.p. 87°C. – ^{1}H NMR (80 MHz, $CDCl_3$): δ = 2.21 (s; 3H), 2.46 (s, br; 8H), 3.75 (s; 6H), 6.79 and 7.14 (mc, AA'BB'; 8H). – MS: *m/z* = 311 (M^+).

$C_{20}H_{25}NO_2$ (311.4) Calcd. C 77.14 H 8.09 N 4.50 Found C 77.26 H 8.02 N 4.81

4,4-Bis(4-methoxy-3,5-dimethylphenyl)-N-methylpiperidine (**17b**): Prepared according to the procedure described for **17a**. Starting from 4.0 g (10.1 mmol) of **16b**, chromatography of the crude product after work up of the Eschweiler-Clarke methylation yielded 2.1 g (56%) of **17b** as colourless glass. – ^{1}H NMR (80 MHz, $CDCl_3$): δ = 2.20 (s; 3H), 2.22 (s; 12H), 2.40 (s, br; 8H), 3.68 (s; 6H), 6.85 (s; 4H). – MS: *m/z* = 367 (M^+).

$C_{24}H_{33}NO_2$ (367.5) Calcd. C 78.43 H 9.05 N 3.81 Found C 78.55 H 9.06 N 3.83

4,4-Bis(4-methoxyphenyl)-N,N-dimethylpiperidinium Fluorosulfonate (**14a**): 1.09 g (0.77 ml, 9.60 mmol) of methyl fluorosulfonate was added via syringe to 1.0 g (3.2 mmol) of **17a** in 20 ml of dry chloroform. After stirring under N_2 for 14 h at room temperature, 100 ml of ether was added. The product, which had precipitated upon standing of the solution at

−30°C, was isolated by filtration, washed with ether and recrystallized from methanol/ether. After drying at 100°C/10^{-3} Torr, 850 mg (62%) of **14a** was obtained, m.p. 194°C.

$C_{21}H_{28}FNO_5S$ (425.5) Calcd. C 59.28 H 6.63 N 3.29 S 7.54
Found C 59.31 H 6.53 N 3.21 S 7.64

4,4-Bis(4-methoxy-3,5-dimethylphenyl)-N,N-dimethylpiperidinium Fluorosulfonate (**15a**): Prepared according to the procedure for **14a**. 1.0 g (2.72 mmol) of **17b** yielded 900 mg (69%) of **15a**, m.p. 189°C.

$C_{25}H_{36}FNO_5S$ (481.6) Calcd. C 62.35 H 7.53 N 2.91 S 6.66
Found C 62.20 H 7.61 N 2.89 S 6.44

4,4-Bis(4-methoxyphenyl)-N,N-dimethylpiperidinium Tetrafluoroborate (**14b**): 5 ml of an aqueous solution of sodium tetrafluoroborate, saturated at 100°C, was added to 200 mg (0.47 mmol) of **14a** in 2 ml of water. After cooling in the refrigerator, the precipitated product was collected by filtration, recrystallized from acetonitrile/ethanol and dried at 100°C/10^{-3} Torr: 150 mg (77%) of **14b**, m.p. 202°C.

$C_{21}H_{28}BF_4NO_2$ (413.2) Calcd. C 61.03 H 6.83 B 2.62 N 3.39
Found C 61.04 H 7.02 B 2.68 N 3.37

4,4-Bis(4-methoxy-3,5-dimethylphenyl)-N,N-dimethylpiperidinium Tetrafluoroborate (**15b**): Prepared according to the procedure described for **14b**. 200 mg (0.415 mmol) of **15a** yielded 125 mg (64%) of **15b**, m.p. 198°C.

$C_{25}H_{36}BF_4NO_2$ (469.4) Calcd. C 63.97 H 7.73 B 2.30 N 2.98
Found C 63.99 H 7.70 B 2.22 N 3.13

4,4-Bis(4-methoxyphenyl)-N,N-dimethylpiperidinium Chloride (**14c**): Prepared according to the procedure described for **1c**–**8c**. 450 mg (1.06 mmol) of **14a** afforded 290 mg (76%) of **14c**, m.p. 259–263°C (dec.). – ^{1}H NMR (80 MHz, D_2O, TSP ext.; [**14c**] = $1.0 \cdot 10^{-3}$ mol · l^{-1}): δ = 2.76 (mc; 4H), 3.14 (s; 6H), 3.44 (mc; 4H), 3.81 (s; 6H), 6.98 and 7.37 (mc, AA′BB′; 8H).

$C_{21}H_{28}ClNO_2$ (361.9) Calcd. C 69.69 H 7.80 Cl 9.80 N 3.87
Found C 69.93 H 7.98 Cl 9.92 N 3.91

4,4-Bis(4-methoxy-3,5-dimethylphenyl)-N,N-dimethylpiperidinium Chloride (**15c**): Prepared according to the procedure described for **1c**–**8c**. 700 mg (1.45 mmol) of **15a** afforded 470 mg (74%) of **15c**, m.p. 228°C (dec.). – ^{1}H NMR see General Part.

$C_{25}H_{36}ClNO_2 \times 1H_2O$ (436.0) Calcd. C 68.86 H 8.78 Cl 8.13 N 3.21
Found C 69.06 H 8.54 Cl 8.12 N 3.33

[1] *F. Diederich* and *K. Dick*, Tetrahedron Lett. **23**, 3167 (1982).
[2] [2a] *F. Diederich* and *K. Dick*, Angew. Chem. **95**, 730 (1983); Angew. Chem., Int. Ed. Engl. **22**, 715 (1983); Angew. Chem. Suppl. **1983**, 957. – [2b] *F. Diederich* and *K. Dick*, J. Am. Chem. Soc. **106**, 8024 (1984). – [2c] *F. Diederich* and *D. Griebel*, J. Am. Chem. Soc. **106**, 8037 (1984).
[3] *F. Diederich* and *K. Dick*, Angew. Chem. **96**, 789 (1984); Angew. Chem., Int. Ed. Engl. **23**, 810 (1984).
[4] *F. Diederich*, Nachr. Chem. Techn. Lab. **32**, 787 (1984).
[5] *Y. Murakami*, Top. Curr. Chem. **115**, 107 (1983).
[6] *I. Tabushi* and *K. Yamamura*, Top. Curr. Chem. **113**, 145 (1983).
[7] *K. Odashima* and *K. Koga*, in Cyclophanes (*P. M. Keehn* and *S. M. Rosenfeld*), Vol. II, pp. 629–678, Academic Press, New York 1983.
[8] *W. Kauzmann*, Adv. Protein Chem. **14**, 1 (1959).
[9] *H. A. Scheraga*, Acc. Chem. Res. **12**, 7 (1979).
[10] *C. Tanford*, The Hydrophobic Effect: Formation of Micelles and Biological Membranes, 2nd ed., Wiley, New York 1980.
[11] *M. L. Bender* and *M. Komiyama*, Cyclodextrin Chemistry, Springer, Berlin 1978.

[12] *W. Saenger*, Angew. Chem. **92**, 343 (1980); Angew. Chem., Int. Ed. Engl. **19**, 344 (1980).
[13] *R. Breslow*, Chem. Br. **19**, 126 (1983).
[14] *I. Tabushi*, Acc. Chem. Res. **15**, 66 (1982).
[15] [15a] *K. Odashima, A. Itai, Y. Iitaka*, and *K. Koga*, J. Am. Chem. Soc. **102**, 2504 (1980). – [15b] *K. Odashima, A. Itai, Y. Iitaka, Y. Arata*, and *K. Koga*, Tetrahedron Lett. **21**, 4347 (1980).
[16] *B. J. Van Keulen, R. M. Kellogg*, and *O. Piepers*, J. Chem. Soc., Chem. Commun. **1979**, 285.
[17] For related approaches see ref.[5,6]; see also [17a] *E. T. Jarvi* and *H. W. Whitlock, jr.*, J. Am. Chem. Soc. **102**, 657 (1980). – [17b] *S. P. Adams* and *H. W. Whitlock, jr.*, J. Am. Chem. Soc. **104**, 1602 (1982). – [17c] *E. T. Jarvi* and *H. W. Whitlock, jr.*, J. Am. Chem. Soc. **104**, 7196 (1982).
[18] *K.-D. Bode*, in Methoden der organischen Chemie (*Houben-Weyl-Müller*), 4th ed., Vol. VI/1c, Part II, pp. 1021–1030, Thieme, Stuttgart 1976.
[19] *P. W. Vittum* and *G. H. Brown*, J. Am. Chem. Soc. **71**, 2287 (1949).
[20] *M. E. McGreal, V. Niederl* and *J. B. Niederl*, J. Am. Chem. Soc. **61**, 345 (1939).
[21] The synthesis of **20** in low yield (1.2%) by a different approach has been previously reported: *S. Smolinski, I. Deja*, and *J. Nowicka*, Tetrahedron **31**, 1527 (1975); Zesz. Nauk Uniw. Jagiellon., Pr. Chem. **20**, 71 (1975) [Chem. Abstr. **84**, 135615j (1976)].
[22] *C. Krieger* and *F. Diederich*, Chem. Ber. **118**, 3620 (1985), following.
[23] In the field of macrocyclic cation-complexation, CPK molecular models have been extensively used in the design of complexes. In most cases, the crystal structures were found to be close to what was anticipated by model examination; see: [23a] *D. J. Cram*, in Applications of Biochemical Systems in Organic Chemistry (*J. B. Jones, C. J. Sih*, and *D. Perlman*); Techniques in Chemistry (*A. Weissberger*), Vol. 10, Part II, pp. 815–873, Wiley, New York 1976. – [23b] *D. J. Cram* and *K. N. Trueblood*, Top. Curr. Chem. **98**, 43 (1981).
[24] *P. Laszlo*, in Progress in NMR Spectroscopy (*J. W. Emsley, J. Feeney*, and *L. H. Sutcliffe*), Vol. 3, pp. 231–402, Pergamon Press, Oxford 1967.
[25] *J. Ronayne* and *D. H. Williams*, in Annual Review of NMR Spectroscopy (*E. F. Mooney*), Vol. 2, pp. 83–124, Academic Press, London 1969.
[26] [26a] *J. H. Bowie, J. Ronayne*, and *D. H. Williams*, J. Chem. Soc. B **1966**, 785. – [26b] *J. H. Bowie, J. Ronayne*, and *D. H. Williams*, J. Chem. Soc. B **1967**, 535. – [26c] *J. Ronayne* and *D. H. Williams*, J. Chem. Soc. B **1967**, 540.
[27] *J. H. Fendler* and *E. J. Fendler*, Catalysis in Micellar and Macromolecular Systems, Academic Press, New York 1975.
[28] *J. H. Fendler*, Membrane Mimetic Chemistry, Wiley New York 1982.
[29] *B. Lindman* and *H. Wennerström*, Top. Curr. Chem. **87**, 1 (1980).
[30] For the determination of critical micelle concentrations by NMR spectroscopy see for example: *E. J. Fendler, U. G. Constien*, and *J. H. Fendler*, J. Phys. Chem. **79**, 917 (1975).
[31] Upon consideration of additional NMR spectra in the low concentration range, the CMC-value of **3c** given in ref.[1] [$(2.5 \pm 0.8) \cdot 10^{-4}$ mol $\cdot$ l^{-1}] had to be corrected to $1.6 \cdot 10^{-4}$ mol $\cdot$ l^{-1}.
[32] [32a] *W. O. McClure* and *G. M. Edelman*, Biochemistry **5**, 1908 (1966). – [32b] *G. M. Edelman* and *W. O. McClure*, Acc. Chem. Res. **1**, 65 (1968).
[33] *H. A. Benesi* and *J. H. Hildebrand*, J. Am. Chem. Soc. **71**, 2703 (1949).
[34] *H. Kondo, H. Nakatani*, and *K. Hiromi*, J. Biochem. **79**, 393 (1976).
[35] For the 1:1 complex between β-CD and methyl anthranilate K_a = 92 l $\cdot$ mol^{-1} was obtained by fluorescence titration: *A. De Korte, R. Langlois*, and *C. R. Cantor*, Biopolymers **19**, 1281 (1980).
[36] *R. J. Bergeron* and *W. P. Roberts*, Anal. Biochem. **90**, 844 (1978).
[37] The + signal refers to a shift to higher magnetic field. $\Delta\delta$ (ppm) = δ of pure host or pure guest in solution – δ of host or guest in the solution of complex.
[38] The signals of 3,4,5,6,7,8-H of **32c** in the solution of complex collapse between δ = 7.45–7.75.
[39] [39a] *W. B. Dandliker* and *V. A. De Saussure*, in The Chemistry of Biosurfaces (*M. L. Hair*), Vol. 1, pp. 1–43, Marcel Dekker, New York 1971. – [39b] *A. Ben-Naim*, Hydrophobic Interactions, Plenum Press, New York 1980.
[40] *A. J. Gordon* and *R. A. Ford*, The Chemists Companion, p. 303, Wiley, New York 1972.

[317/84]